NAVAL SHIP RESEARCH AND DEVELOPMENT CENTER
Bethesda, Md. 20034

WALL SHEAR STRESS AND MEAN-VELOCITY MEASUREMENTS IN A THREE-DIMENSIONAL TURBULENT BOUNDARY LAYER

by

John L. Power

SHIP PERFORMANCE DEPARTMENT
RESEARCH AND DEVELOPMENT REPORT

September 1973 Report 4056

Report 4056
WALL SHEAR STRESS AND MEAN-VELOCITY MEASUREMENTS IN A THREE-DIMENSIONAL TURBULENT BOUNDARY LAYER

The Naval Ship Research and Development Center is a U. S. Navy center for laboratory effort directed at achieving improved sea and air vehicles. It was formed in March 1967 by merging the David Taylor Model Basin at Carderock, Maryland with the Marine Engineering Laboratory at Annapolis, Maryland.

Naval Ship Research and Development Center
Bethesda, Md. 20034

MAJOR NSRDC ORGANIZATIONAL COMPONENTS

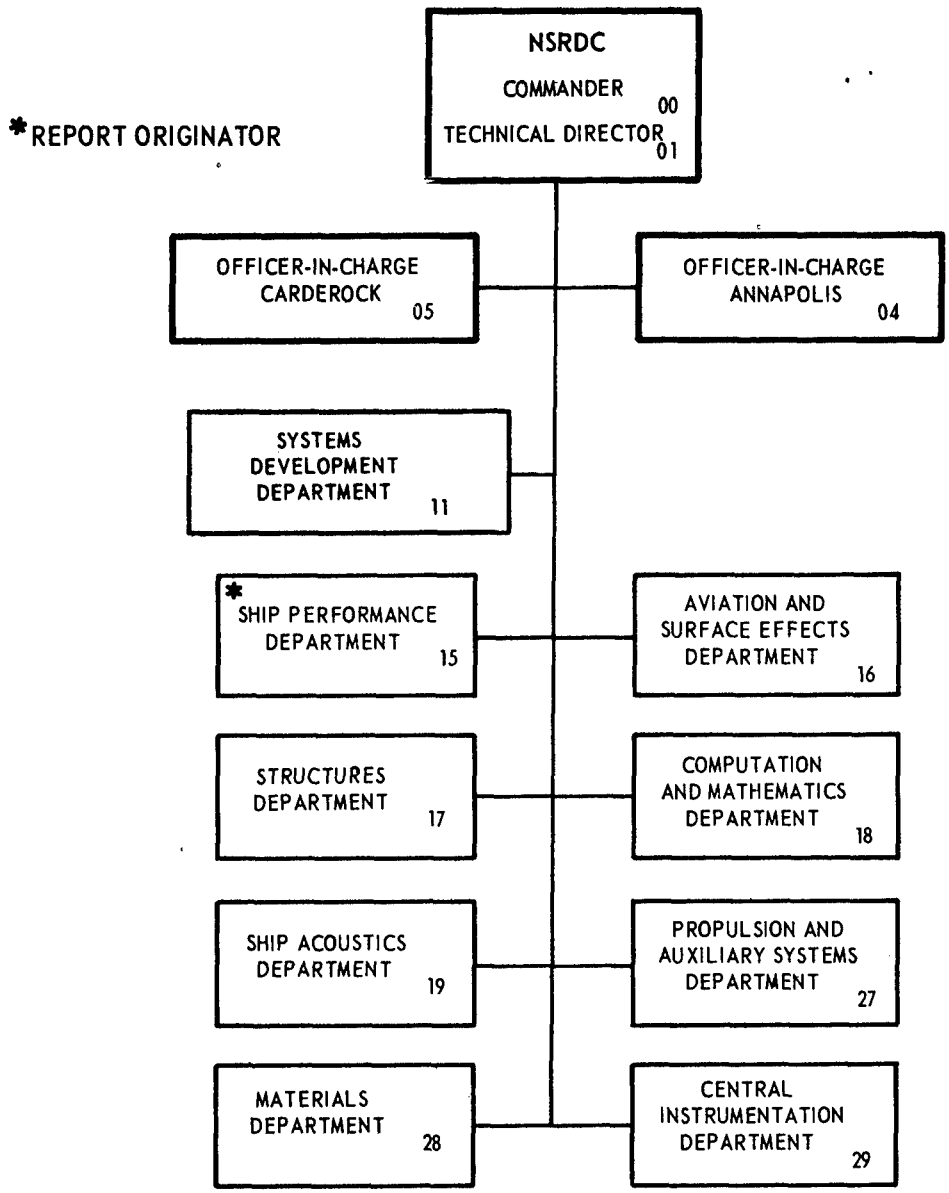

NDW-NSRDC 3960/43b (Rev. 3-72)
GPO 928-108

DEPARTMENT OF THE NAVY
NAVAL SHIP RESEARCH AND DEVELOPMENT CENTER
BETHESDA, MARYLAND 20034

WALL SHEAR STRESS AND MEAN-VELOCITY MEASUREMENTS IN A THREE-DIMENSIONAL TURBULENT BOUNDARY LAYER

by

John L. Power

September 1973

Report 4056

TABLE OF CONTENTS

LIST OF FIGURES

PAGE

LIST OF TABLES

PAGE

NOTATION

c_w	Wall friction coefficient $\tau_w/1/2\,\rho U_1^2$
c_{w_1}	Wall friction coefficient in inviscid streamline direction
H	Shape factor δ_1/θ_{11}
Ho	Quantity defined in Equation (7)
p_L	Pressure in left tube of pressure probe
p_R	Pressure in right tube of pressure probe
p_i	Pressure in tunnel test section
p_o	Pressure at tunnel test-section entrance
Q, Q_o	Quantities defined in Equation (7)
$R_{\delta 1}$	Reynolds number $U_1\,\delta_1/\nu$
$R_{\theta 11}$	Reynolds number $U_1\,\theta_{11}/\nu$
U	Velocity in boundary layer in direction of inviscid streamline at edge of boundary layer
$\vec{U}$	Velocity vector in boundary layer
U_l	Velocity at edge of boundary layer
U_m	Velocity sensed by impact tube
U_o	Free-stream velocity at tunnel test-section entrance; also, jet velocity of calibration tunnel
u_τ	Friction velocity $\sqrt{\tau_w/\rho}$
W	Velocity in boundary layer perpendicular to inviscid streamline direction

y	Perpendicular distance from tunnel floor
α	Probe angle of attack
β	Angle U makes with inviscid streamline direction
β_o	Value of β as y approaches zero
Δp_m	Pressure imbalance in impact tube of pressure probe
Δp_s	Pressure imbalance in side tubes of pressure probe
δ	Boundary layer thickness
$\delta_1, \delta_2, \theta_{11}$ $\theta_{12}, \theta_{21}, \theta_{22}$	Boundary layer integral thicknesses defined in text
ν	Kinematic viscosity of fluid
ρ	Density of fluid
τ_w	Wall shear stress

ABSTRACT

A three-dimensional smooth wall turbulent boundary layer with a moderate adverse pressure gradient was produced on the floor of a wind tunnel. The boundary layer velocity profile was measured at two positions, using a three-tube pressure probe. The streamwise, skin-friction coefficient was calculated with the skin-friction laws of Granville and Ludwieg and Tillmann using experimentally obtained boundary layer parameters. The results were compared with skin-friction coefficients obtained by using Preston tubes.

The calculated values of skin friction varied from agreement to 5 percent more than the Preston tube values. There is also evidence that the skewed flow in the boundary layer can affect Preston tube readings. It was concluded that the tunnel could be used to study boundary layers similar to those occurring on ships of moderate block coefficient.

ADMINISTRATIVE INFORMATION

This research was supported by the General Hydromechanics Research Program under S-R023 01 01, Task 00104, Work Unit 552-110.

INTRODUCTION

The ability to calculate total resistance of ship hulls is of obvious importance to the Navy. An important component of this resistance is the drag due to skin friction. To be able to predict skin friction requires the ability to calculate the properties of three-dimensional, turbulent-boundary layers. Existing methods for three-dimensional, turbulent boundary-layer calculations consist of two approaches: (1) momentum integral, and (2) differential. For an example of a momentum integral method, see Reference 1* and for an example of a differential method, see Reference 2. As with all computations of turbulent boundary layers, both methods require some empirical input. Because of the lack of three-dimensional data, recourse must often be made to two-dimensional empirical formulations. There is a need for experimental three-dimensional data to provide the empirical input for three-dimensional calculations, to check the validity of the calculations, and to determine when the use of two-dimensional formulations is valid.

Much of the existing three-dimensional data have been obtained using swept wings. The source of most of these data is referenced by Nash and Patel[3] in their review of the current state of three-dimensional

[1]Cumpsty, N.A. and M.R. Head, "The Calculation of Three-Dimensional Turbulent Boundary Layers, Part 1: Flow Over the Rear of an Infinite Swept Wing," The Aeronautical Quarterly, Vol. 18 (1967).
*A complete listing of references is given on page 37.

[2]Bradshaw, P., "The Calculation of Three-Dimensional Turbulent Boundary Layers," Journal of Fluid Mechanics, Vol.46, Part 3 (1971).

[3]Nash, John T. and V.C. Patel, "Three-Dimensional Turbulent Boundary Layers," SEC Technical Books, Scientific and Business Consultants, Inc., Atlanta, Ga. (1972).

boundary-layer work. This type of flow is different from and more restricted than flow over a ship hull in that the flow properties are identical in all planes normal to the axis of the wing. The Johnston[4] study of the flow over a swept forward-facing step would also fall into this flow category.

Experimenters have used various devices to create more general three-dimensional boundary layers for experimental investigations. East and Hoxey[5] and Hornung and Jourbert[6] used cylinders mounted in two-dimensional, flat-plate boundary layers with the cylinders axes perpendicular to the plate. Grunschwitz[7] and Francis and Pierce[8] used curved internal channels with large potential cores to create secondary flow. Johnston[9] used a retangular jet stagnating against a wall. In all of these experiments, the boundary layer was dominated by the external pressure gradients; in the outer wake region, the shear effects were small when compared to inertial effects.

This report describes the first year of progress of an exploratory program for obtaining experimental three-dimensional, boundary-layer data at the Center. The goal has been to obtain and investigate boundary layers whose properties approximate boundary layers usually found on ships. With some exceptions, ship boundary layers are characterized by large radii of curvature and small pressure gradients in the transverse direction. Thus, pressure effects do not dominate, and inertial and shear stress effects are both important in the boundary-layer wake region. The facility chosen to duplicate these conditions was a wind tunnel with flexible sidewalls. Measurements have been made on the floor of the tunnel, and three-dimensional effects have been obtained from transverse pressure gradients created by curving the walls. Longitudinal pressure gradients along the tunnel can also be created by varying the distance between the walls, simulating this property of flow about ships.

Momentum integral calculation methods require empirical input from the vector mean-velocity profiles of the boundary layer. The differential methods require, in addition, vector profiles of the turbulent shear stress. Experimental mean velocity profiles can be obtained with either pressure probes or hot wires. To obtain the shear-stress profile is more difficult and requires using an X hot wire probe and associated electronic equipment. To date this program has been limited to obtaining the characteristics of a three-tube pressure probe and to making two mean-velocity surveys on a smooth wall with this probe for one tunnel geometry. Skin friction at the survey positions was obtained with Preston tubes. The results of these tests, together with a description of the facility, probes, and instrumentation used, make up the bulk of this report.

---

[4]Johnston, J.P., "Measurements in a Three-Dimensional Turbulent Boundary Layer Induced by a Swept, Forward-Facing Step," Journal of Fluid Mechanics, Vol. 42, Part 4, pp. 823-844 (1970).

[5]East, L.T. and R.P. Hoxey, "Low Speed Three-Dimensional Turbulent Boundary Layer Data," Parts 1 and 2, Aeronautical Research Council, R and M 3653 (1969).

[6]Hornung, H.G. and P.N. Joubert, "The Mean Velocity Profile in Three-Dimensional Turbulent Boundary Layers," Journal of Fluid Mechanics, Vol. 5, Part 3 (1963).

[7]Grunschwitz, E., "Turbulente Reigungsschichten mit Sekundarstromoung," Ingeniuer-Archiv, Vol. VI, (1935).

[8]Francis, G.P. and F.J. Pierce, "An Experimental Study of Skewed Turbulent Boundary Layers in Low Speed Flows," Journal of Basic Engineering, Transactions American Society of Mechanical Engineers, Series D, Vol. 89, No. 3, pp. 597-607 (1967).

[9]Johnston, J.P., "On the Three-Dimensional Turbulent Boundary Layer Generated by Secondary Flow," Journal of Basic Engineering, Transactions American Society of Mechanical Engineers, Series D, Vol. 82, pp. 233-248 (1960).

EXPERIMENT

EXPERIMENTAL APPARATUS

Wind Tunnel

The facility used in these experiments was a low-turbulence wind tunnel, situated at the Center. This tunnel is an open return type, having a test section 14.5 ft long and a 2 ft wide by 4 ft high cross section at both ends. When the sidewalls are kept straight, the test section has a cross section 2 ft wide by 4 ft high. However, both sidewalls are flexible, and each is capable of a maximum displacement of approximately 7 in. in either direction. This allows creation of three-dimensional boundary layers, both with and without longitudinal pressure gradients, on the floor and top of the test section of the tunnel. At maximum power, approximately 150 ft/sec can be obtained with straight sidewalls. The general arrangement of the wind tunnel is shown in Figure 1, and a complete description is given in Reference 10.

Pressure Probes

The velocity magnitude and direction in the boundary layer was measured by a three-tube pressure probe. The two outer tubes were cut back 40 deg to be sensitive to flow direction. The difference in pressure between the two outer tubes has been used to indicate alignment of the probe relative to the velocity direction. The center tube is a conventional impact tube and is used in conjunction with a nearby static hole to measure velocity magnitude. Figure 2 gives construction details of the probe, and Figure 3 is a photograph.

The static pressure was measured by 1/8-in.-dia pressure taps, located at 1-ft intervals along the floor of the tunnel. In addition a static probe was available to survey the static pressure through the boundary layer. This probe has an outside diameter of 0.060 in. with four sensing holes placed concentrically around the circumference, 1 in. from the end of the probe. The diameter of each sensing hole is 0.0135 in.

The free-stream characteristics of the three-tube pressure probe were determined before the wind tunnel tests, using a small calibration tunnel; see Figure 4. The tunnel produced a uniform jet of air, having a cross sectional area of 2 by 2 in. at its exit. The jet velocity is variable from 10 to 130 ft/sec. The probe was placed beside a standard impact tube, and the probe clamping device was mounted to a protractor so that the probe angle of attack could be determined accurately. Using this system, the accuracy, directional sensitivity, and time response of the probe tubes were determined.

Figure 5 gives the directional sensitivity of the two side tubes where p_R is pressure sensed by the right side tube as seen from above, p_L is pressure sensed by the left side tube, ρ is density of the fluid, U_o is calibration tunnel-jet velocity, and α is angle of attack of probe; $\alpha=0$ is defined by $p_R - p_L = 0$,

---

[10]Scottron, V.E. and D.A. Shaffer, "The Low Turbulence Wind Tunnel," David Taylor Model Basin, Report 2116 (Dec 1965).

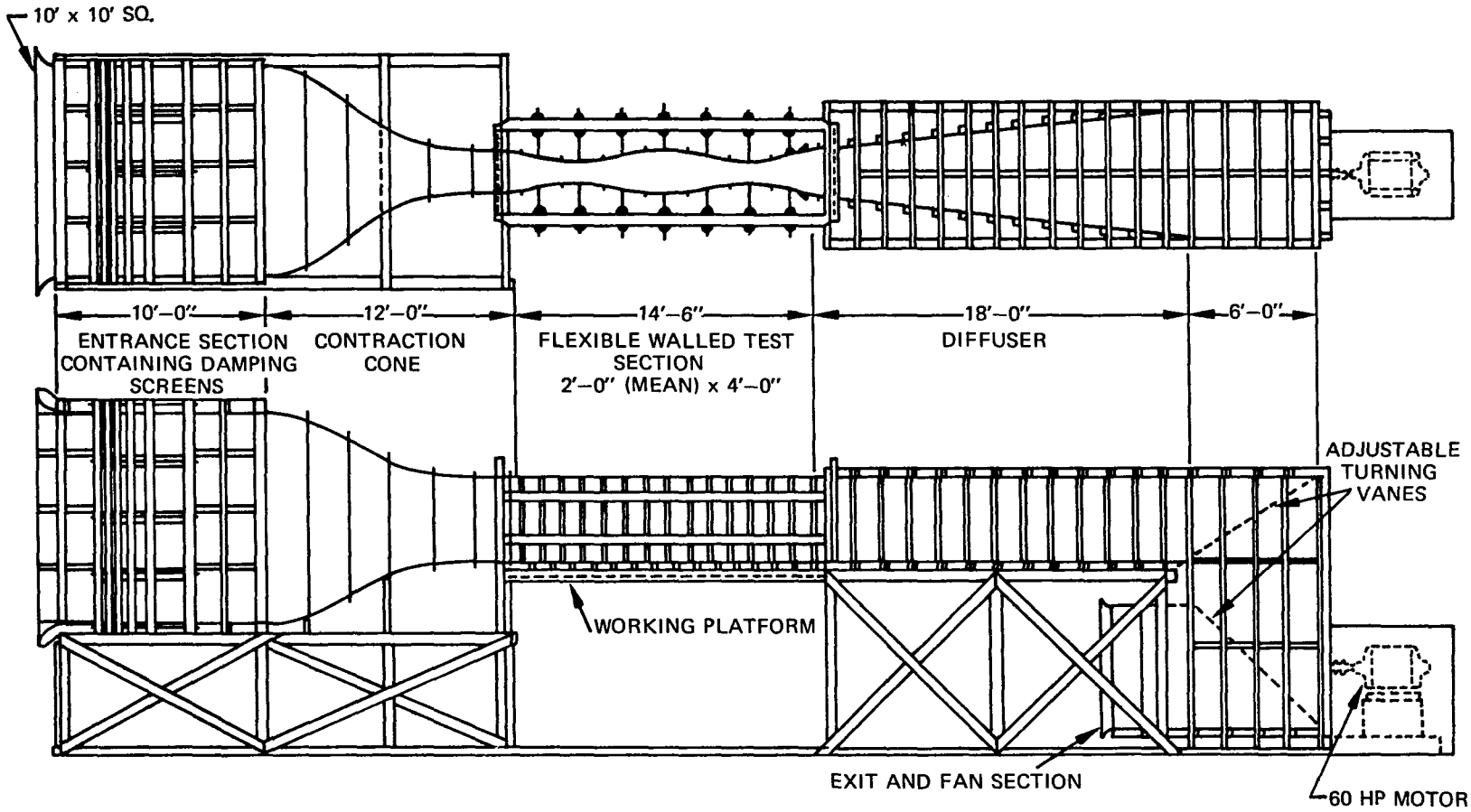

Figure 1 – Arrangement of Wind Tunnel

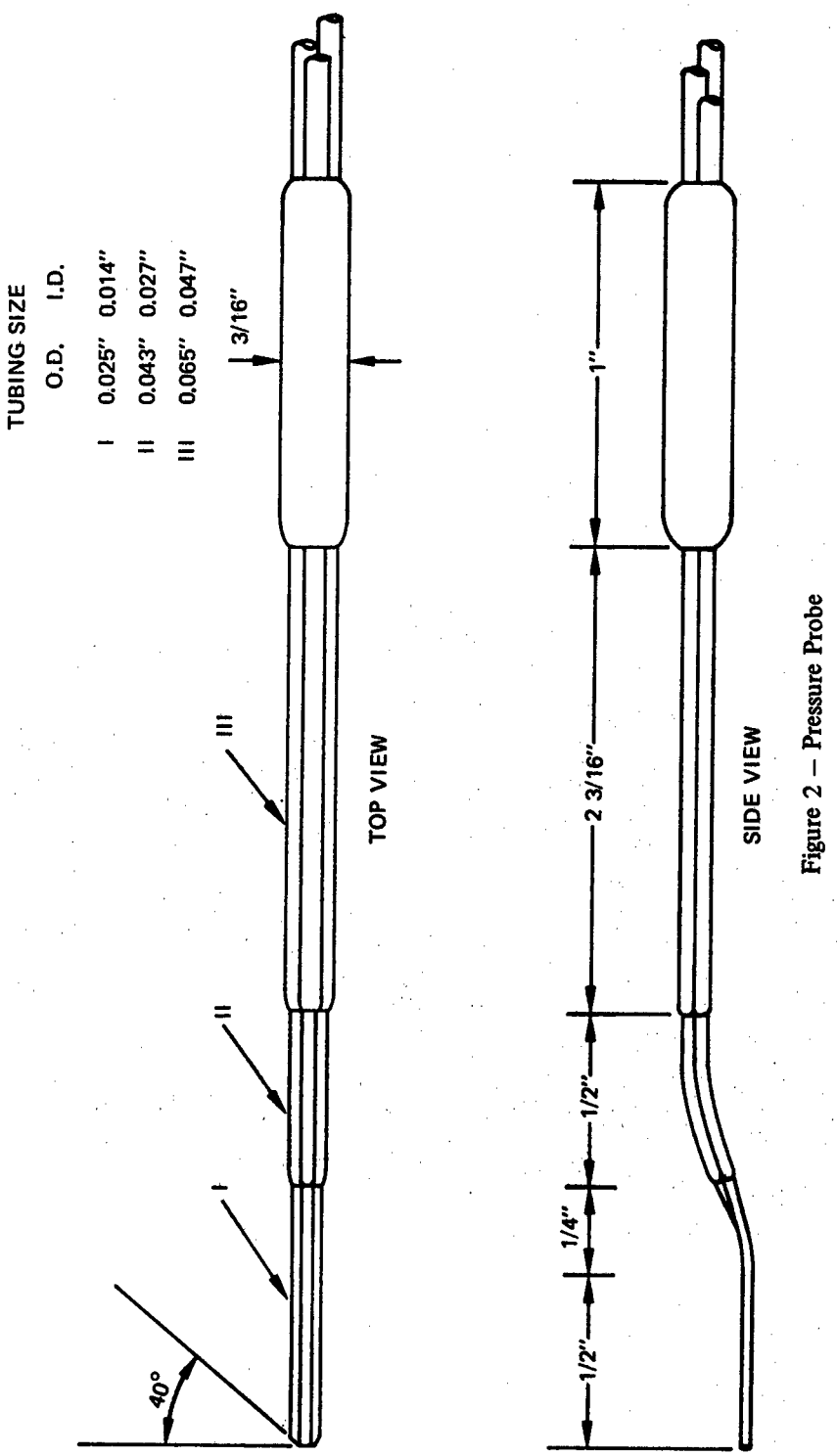

Figure 2 – Pressure Probe

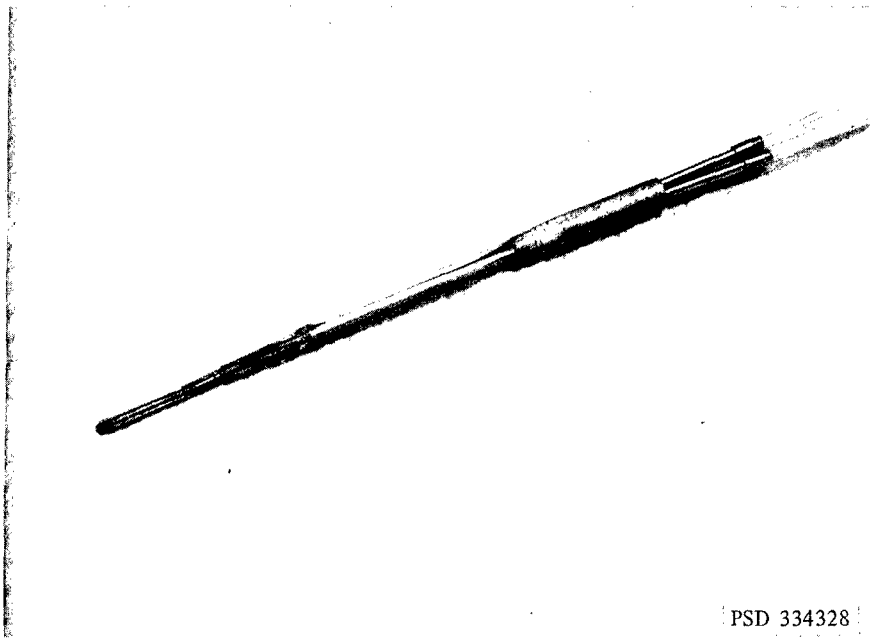

Figure 3 – Directional Pressure Probe

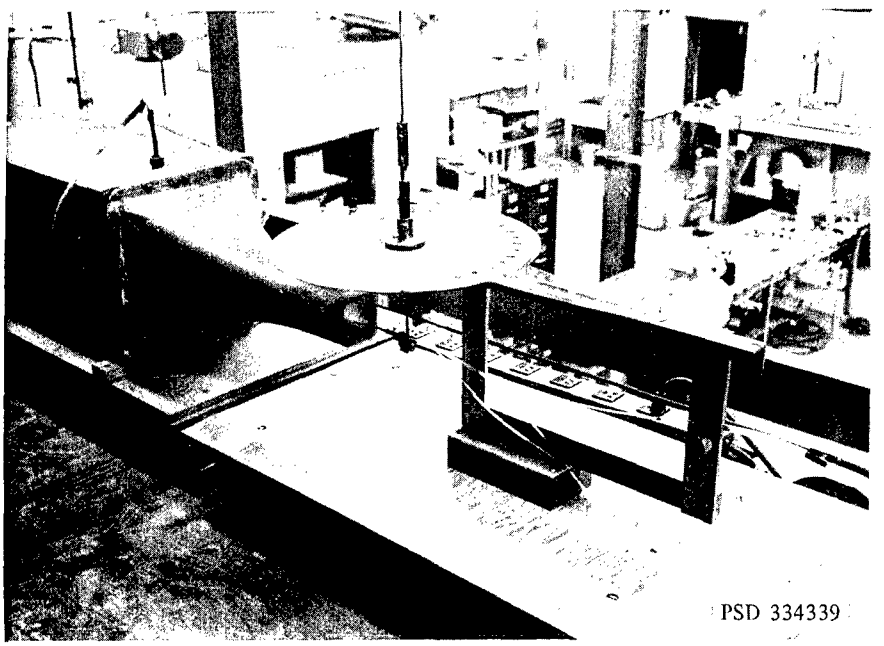

Figure 4 – Exit of Calibration Tunnel

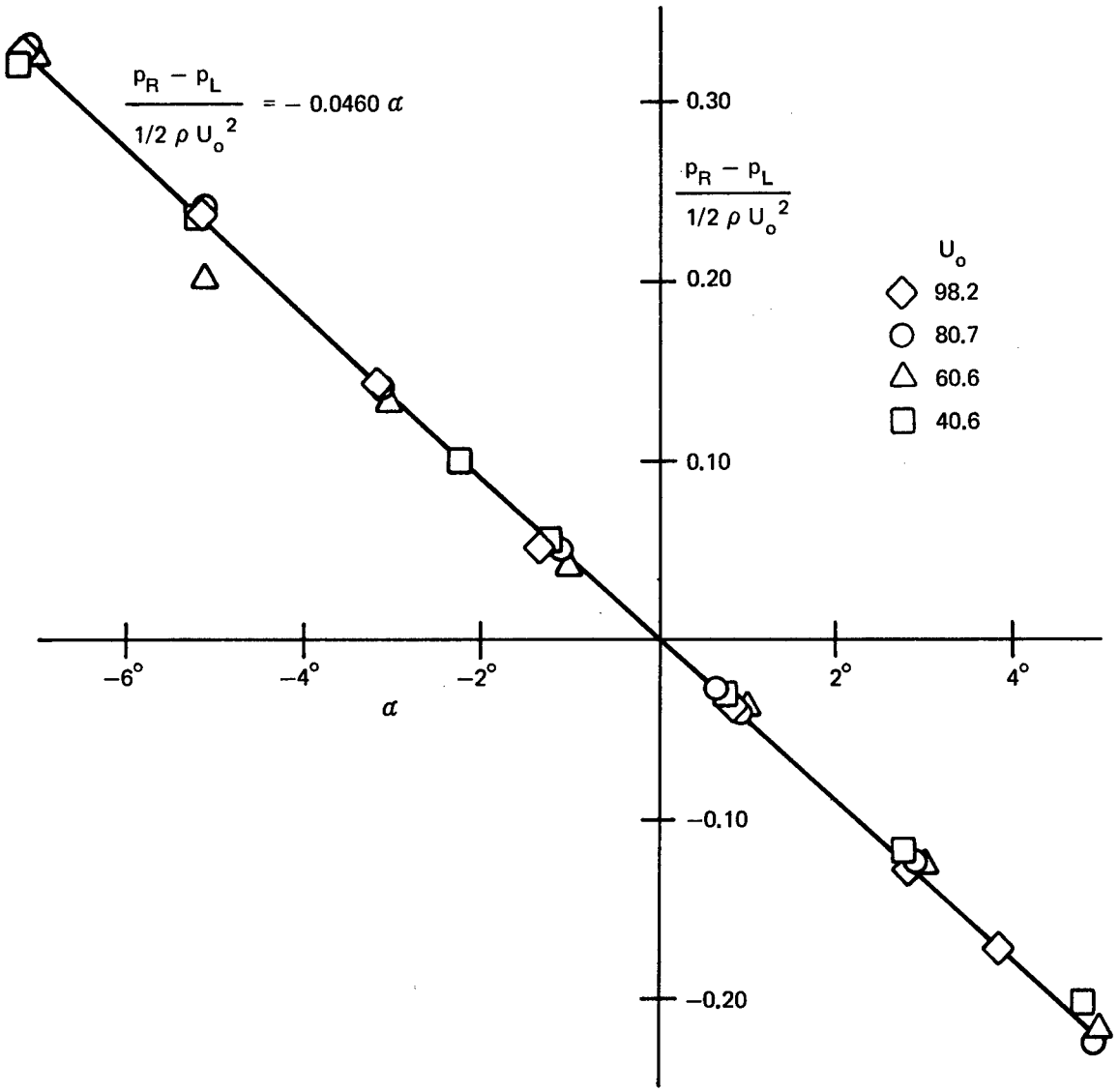

Figure 5 – Directional Sensitivity of Side Tubes of Pressure Probe

positive rotation clockwise when viewed from above. Data were taken at four different calibration-tunnel speeds. The results show that the pressure difference $(p_R - p_L)$ is linear for small values of α, within the accuracy of the measurements, and can be approximated by the equation

$$\frac{p_R - p_L}{1/2\ \rho\ U_o^2} = 0.0460\ \alpha$$

where α is in degrees. This result has been confirmed by data taken later in the wind tunnel that have not been shown in Figure 5.

The time response of the two side tubes is shown in Figure 6. This is the time required for the probe side tubes to reach the equilibrium pressure $p_L - p_R$, associated with the probe angle of attack α as a function of pressure imbalance Δp_s in the side tubes. The results shown on this curve were taken at 40, 60, 80 and 100 ft/sec and at several angles of attack, ranging from $-6^o \leq \alpha \leq 5^o$, and were useful in determining the necessary waiting time for taking data.

The directional sensitivity and time response of the center or impact tube is given in Figures 7 and 8 where

$\alpha = 0$ is defined by the condition $p_R - p_L = 0$

U_m is velocity sensed by impact tube

Δp_m is pressure imbalance in impact tube.

Figure 7 shows the probe has a flat response, within 0.1 percent of maximum reading, when its angle of attack is varied 8 deg, i.e., $-7^o \leq \alpha \leq +1^o$, and that the geometric alignment of the probe differs from the dynamic alignment defined by $p_R - p_L = 0$ by approximately 4.5 deg. The velocity sensed by the pressure probe was also calibrated with a standard probe, using the calibration tunnel. The results showed that over a wide range from 40 to 100 ft/sec, the measured speeds differ by 0.3 percent or less.

Two Preston tubes were used to measure the wall friction. They were made from cylindrical tubing about 6 in. long, were cut square at the end, and were installed by cementing them to the floor with quick-drying epoxy. Their dimensions are given in Table 1.

TABLE 1 – DIMENSIONS OF PRESTON TUBES

Tube	Outside Diameter in.	Inside Diameter in.	Ratio
1	0.065	0.047	0.72
2	0.1255	0.061	0.49

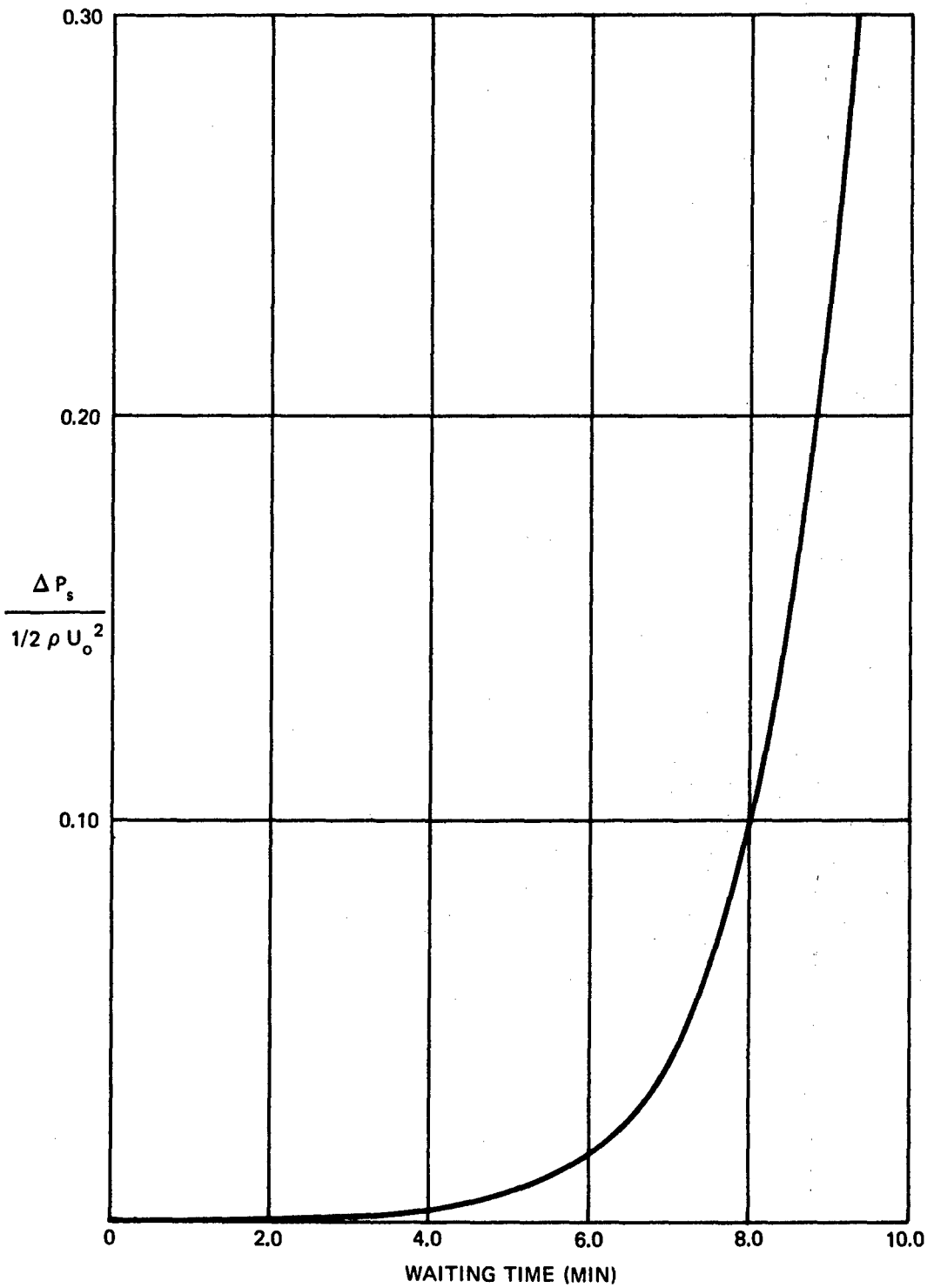

Figure 6 – Time Response of Side Tubes of Pressure Probe

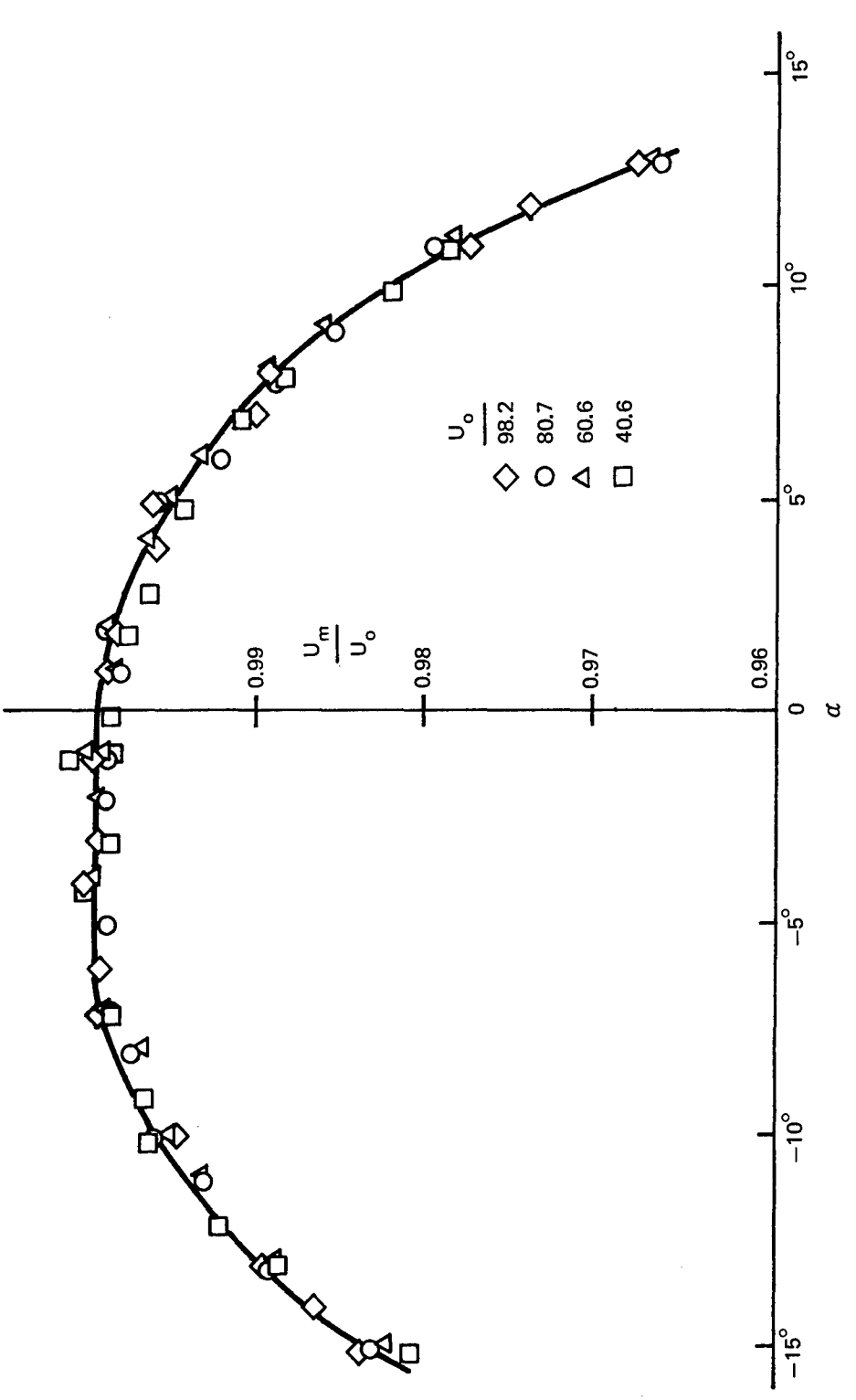

Figure 7 – Directional Sensitivity of Impact Tube of Pressure Probe

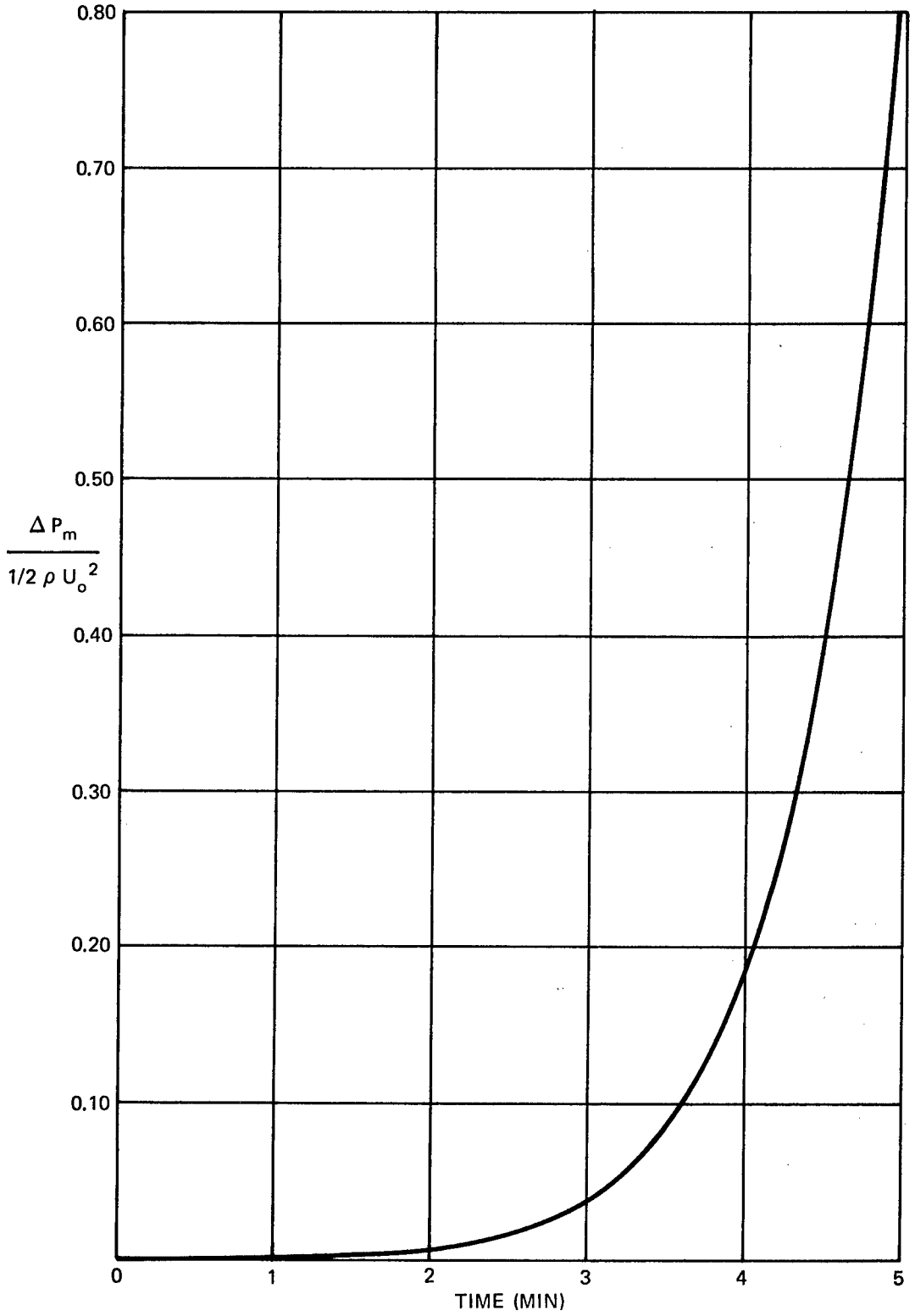

Figure 8 – Time Response of Impact Tube of Pressure Probe

Instrumentation

All pressures were measured by two inclined manometers, having a slope setting of approximately 1:10. These manometers were calibrated at intervals throughout the experiment by a precision micromanometer,[11] having an accuracy of 0.001 in. of fluid. The inclined manometers were graduated for each 0.01 in. of fluid but could be read to accuracies better than 0.005 in. The calibrations indicated considerable deviation of the inclined manometers from a 1:10 slope, and all data taken were corrected for this error. Figures 9 and 10 show an inclined manometer and the micromanometer, respectively. Dow-Corning 200 silicone fluid, having a specific gravity of 0.82, was used as manometer fluid.

Probe Support and Positioning

The tunnel construction dictated that the measurements be made in the boundary layer along the floor. The only feasible access for a boundary-layer survey was through Lucite windows placed every 2 ft along the tunnel top. Figure 11 shows the device used to support and position the probes under these circumstances. The strut had a 4:1 ogival cross section with a 4-in. chord and could be rotated to align with the direction of free-stream flow in the tunnel. Sleeve bearings installed in both ends of the strut provided rigid support but allowed easy vertical movement and rotation of a probe-positioning tube. The details of the lower end of this tube are given in Figure 12. The upper end of the positioning tube was fixed to translate with a protractor plate but could rotate with respect to the plate. The protractor arm was clamped to the positioning tube, and the protractor plate was bolted to a lathe feed which had a movement of 4.5 in. in the vertical direction. The lathe feed and protractor are shown in Figure 13, while Figures 14 and 15 show the strut and installed pressure probe. The lathe feed has a resolution of 0.0005 in.; the protractor, 2 min.

PROCEDURE

For each boundary layer survey, the magnitude of the velocity vector was measured at 30 positions y perpendicular to the floor. The positions were distributed linearly on a logarithmic scale. The procedure used was to determine, first, the velocity direction β at every other position. These results were then used to align the probe properly at the 30 positions for measuring the velocity magnitude.

When measuring the velocity or making Preston tube measurements, the static pressure was measured at the nearest static hole available. This was one of several static holes, located every foot along the floor of the tunnel. At each survey location, the boundary layer was surveyed with the static pressure probe to determine any difference in the static pressure of the boundary layer and the static pressure used in the velocity or Preston tube measurements. When necessary, these measurements were corrected to reflect the difference.

---

[11] Smith, A.M.O. and J.S. Murphy, "Micromanometer for Measuring Boundary Layer Profiles," The Review of Scientific Instruments, Vol. 26, No. 8 (Aug 1955).

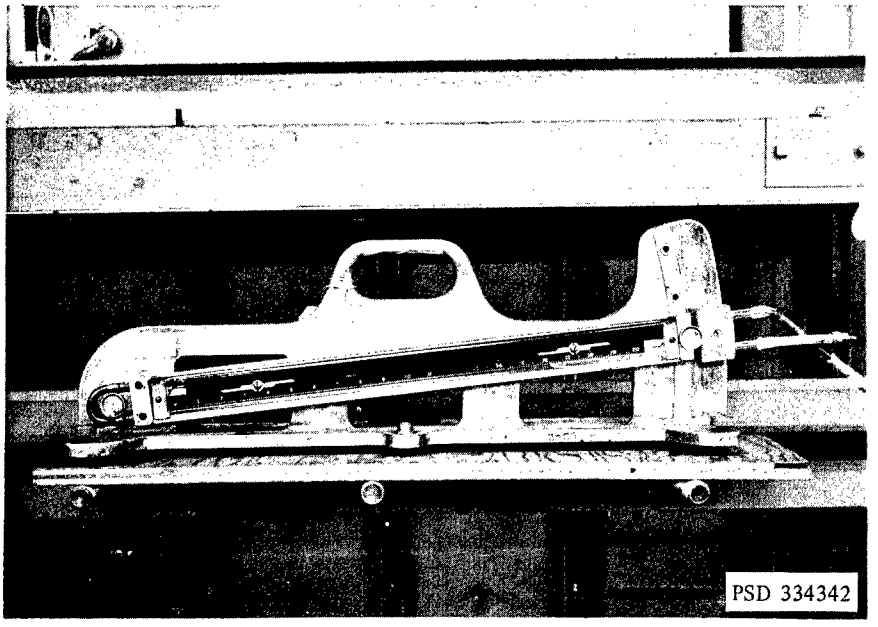

Figure 9 – Inclined Manometer

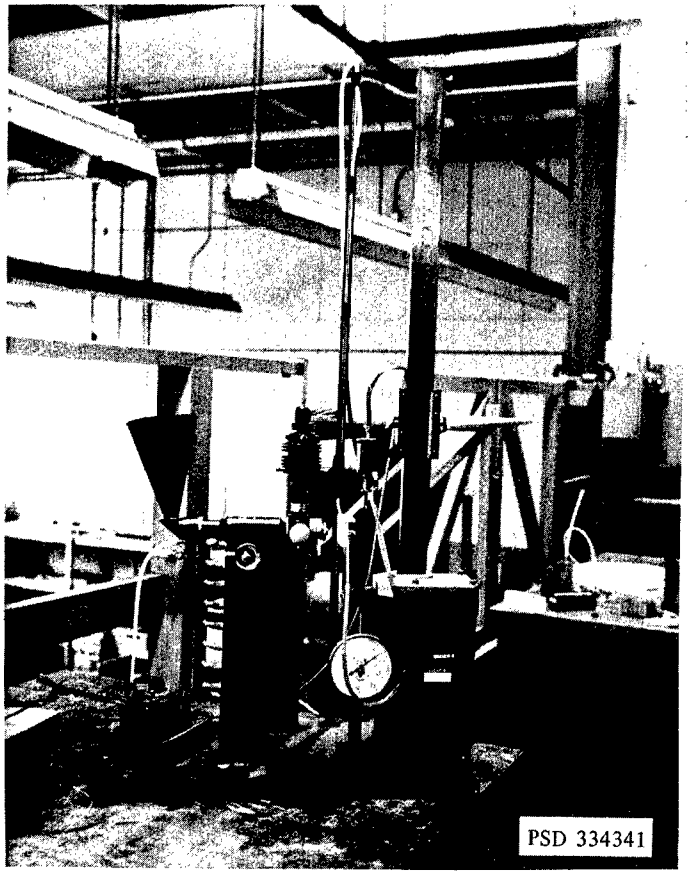

Figure 10 – Micronanometer

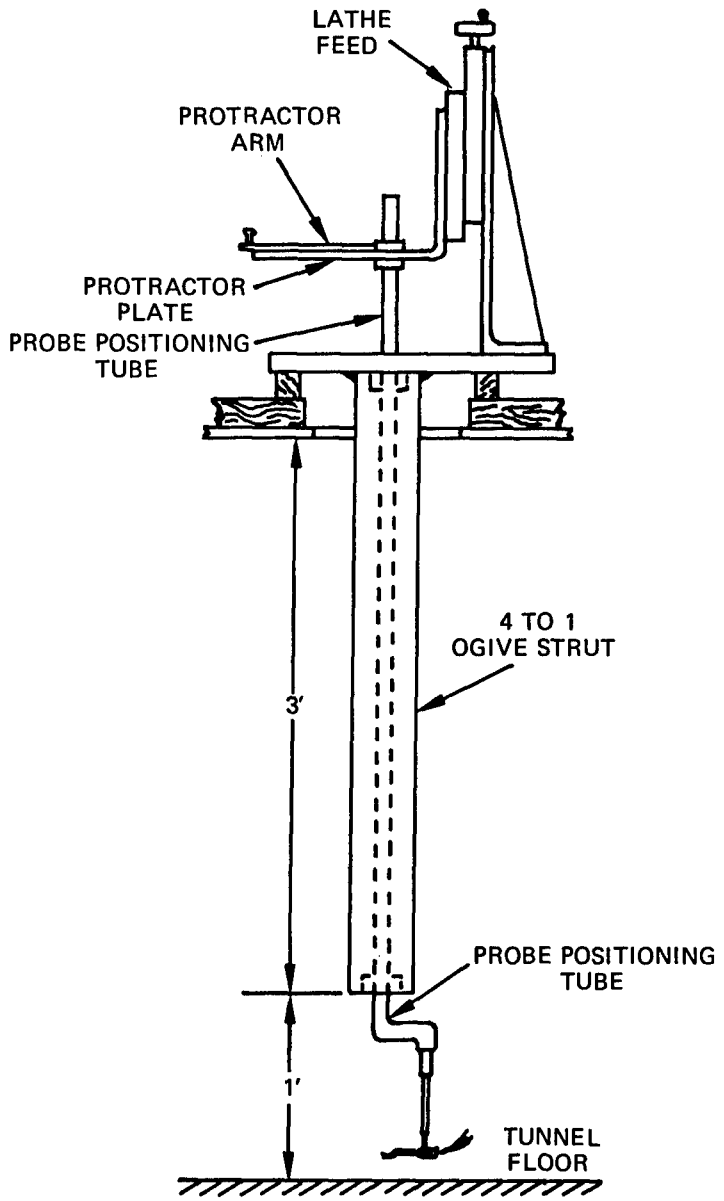

Figure 11 – Probe Support and Positioning Device

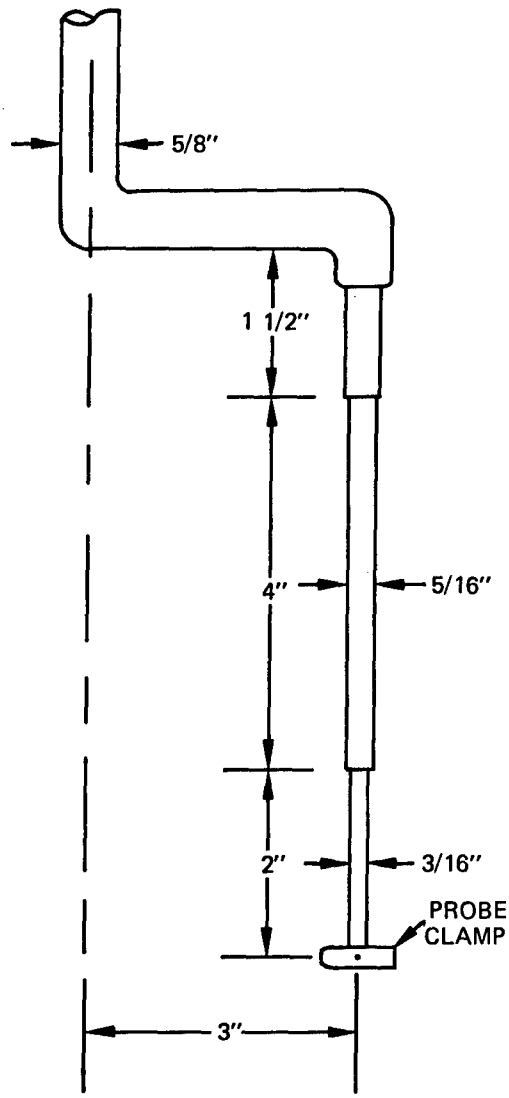

Figure 12 – Lower End of Positioning Tube

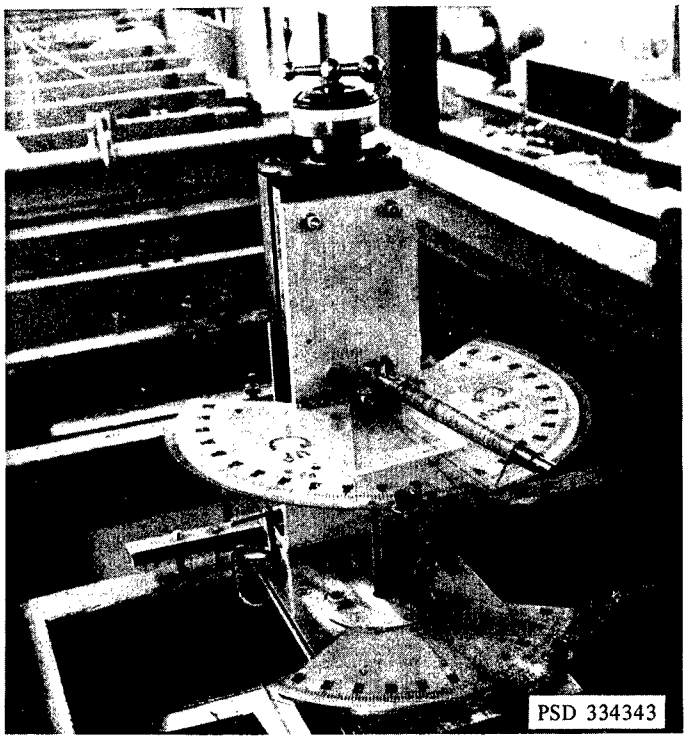

Figure 13 – Lathe Feed and Protractor

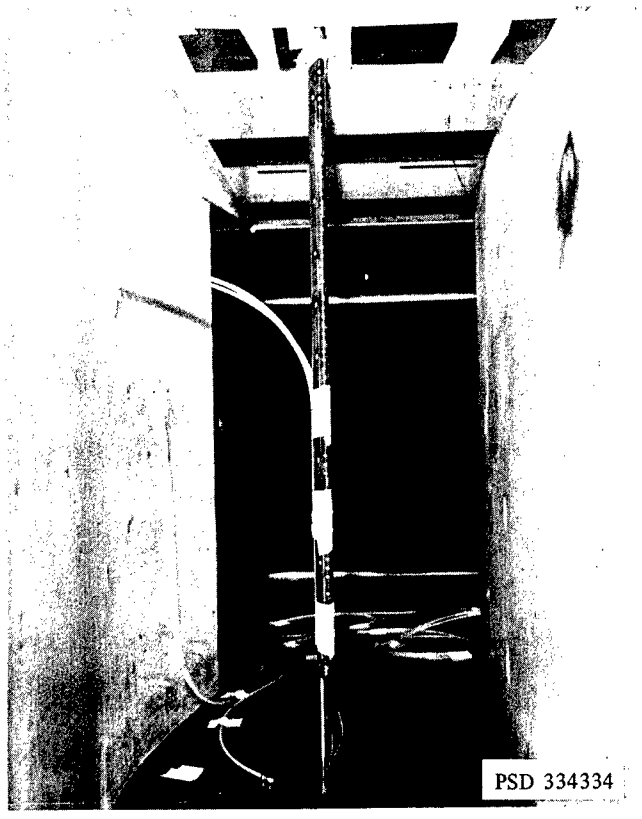

Figure 14 – Strut and Pressure Probe
Installed in Tunnel

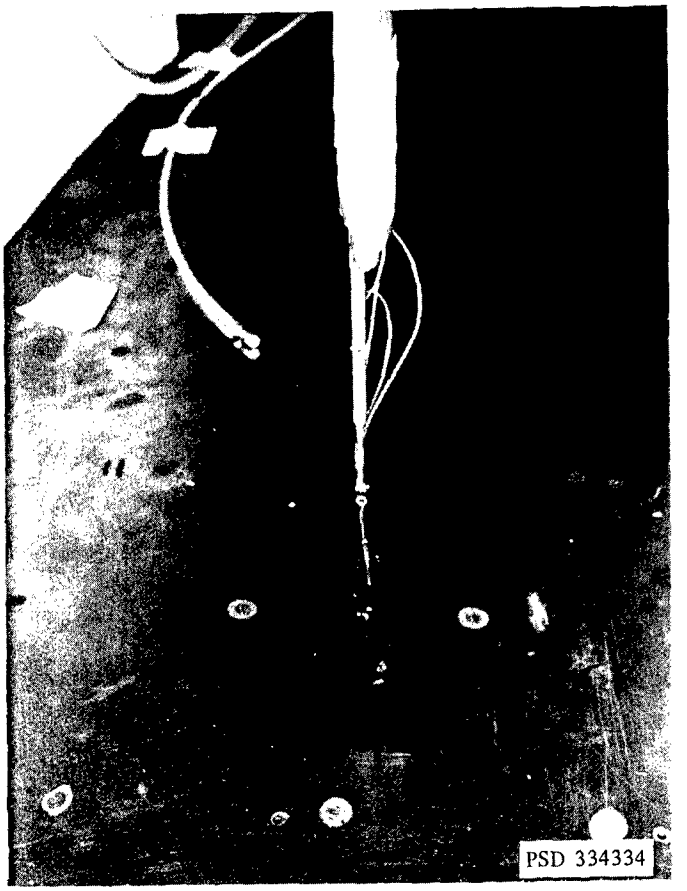

Figure 15 – Lower End of Strut with Pressure Probe Installed

The procedure followed to determine β at a given y was to record the values of $p_R - p_L$ at three values of α close to and bracketing β. The neighborhood of β could be found rapidly by rotating the probe to different positions and watching the reaction of the manometer. The value of β was found by plotting the values of $p_R - p_L$ against α to determine the α at which $p_R - p_L = 0$. The values of β were measured relative to the flow direction at the edge of the boundary layer, positive rotation being clockwise when viewed from above.

The accuracy to which β could be determined depended upon the velocity being sensed by the probe. Figure 16 gives $p_R - p_L$ in inches of Dow-Corning fluid as a function of α for different velocities. The velocities measured during the tests ranged from 33 to 90 ft/sec. For 95 percent of the boundary-layer thickness, β could be determined to the resolution of the protractor, 0.033 deg. Closer to the wall where the velocity was less than 50 ft/sec, the results were not as reliable. About $\alpha = 0$, a pressure change as small as 0.001 in. of fluid could be observed by opening the manometer to atmospheric pressure, switching back to the probe, and observing any movement of the fluid. The direction of the manometer movement gave the sign of α. By using this method, β could be determined with 0.1 deg in all cases.

While the surveys of velocity magnitude were being made, the probe was moved from the inviscid region downward toward the tunnel floor. Thus, the velocity of the inviscid flow at the edge of the boundary layer U_1 was measured at the beginning of the survey. During the survey the tunnel velocity was monitored by maintaining the difference in pressure between a total head tube, located in the tunnel entrance section just downstream of the damping screens, and a static pressure hole at the test section entrance (Figure 1) at a fixed value. If, during a survey, the atmospheric changes were sufficient to appreciably affect the tunnel velocity, the value of U_1, used to nondimensionalize the boundary-layer profiles, was adjusted accordingly.

When the Preston tubes were being used, the velocity, U_1, was determined with the pressure probe mounted at the edge of the boundary layer. The Preston tubes were aligned using reference lines marked on the tunnel floor with the aid of the probe-positioning tube. Wall friction was determined at several speeds that spanned the tunnel speed used for the boundary-layer surveys. The Preston tube data thus obtained were reduced, using a tabulated presentation of the Patel calibration given in Reference 12.

TESTS AND RESULTS

As stated previously, two surveys were made in a three-dimensional boundary layer. Prior to this, velocity surveys were made at one position and two tunnel speeds in a two-dimensional boundary layer (straight tunnel walls.) These tests were made to check the operation of the equipment and of the pressure probes; however, the data have been given for the record. Results of the two-dimensional tests have been given first, and then the three-dimensional results have been presented.

[12]Head, M.R. and V.V. Ram, "Simplified Presentation of Preston Tube Calibration," The Aeronautical Quarterly (Aug 1971).

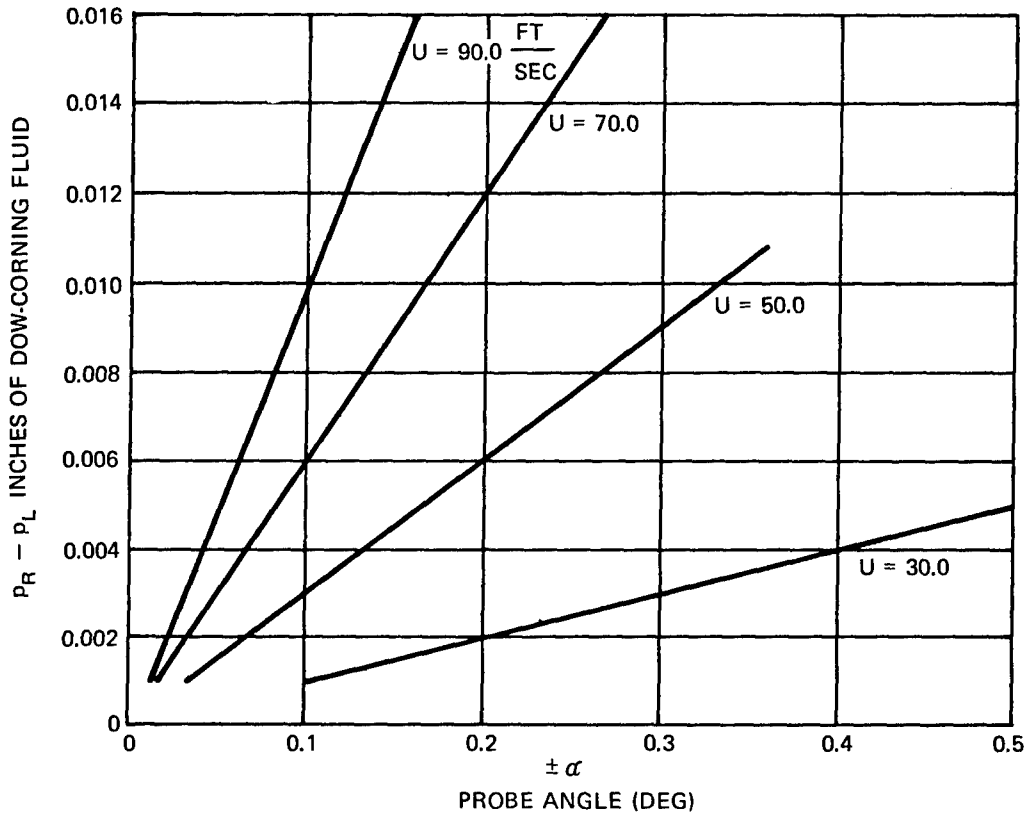

Figure 16 – $p_R - p_L$ in Inches of Dow-Corning Fluid as a Function of Probe Angle of Attack

The notation used to describe the results is as follows:

c_w is wall friction coefficient, $\dfrac{\tau_w}{1/2\ \rho\ U_1^2}$

c_{w_1} is wall friction coefficient in direction of inviscid streamline

$\vec{U}$ is velocity vector in boundary layer

U is velocity in boundary layer in direction of the inviscid streamline at the edge of the boundary layer

U_1 is velocity at edge of boundary layer

U_o is free-stream velocity at test-section entrance

W is velocity in boundary layer perpendicular to direction of inviscid streamling

y is perpendicular distance from tunnel floor

δ is boundary-layer thickness

β is angle $\vec{U}$ makes with direction of inviscid streamline

β_o is value of β as y approaches zero

τ_w is wall friction

ρ is density of fluid

ν is kinematic viscosity of fluid

Results of the boundary-layer surveys have been tabulated and also are presented as plots of velocity versus distance from the wall. No corrections for wall interference or shear flow have been applied to the data. The usual integral thicknesses and the shape factor have been computed from the velocity profiles. These quantities are defined as

$$\delta_1 = \int_o^\delta \left(1 - \frac{U}{U_1}\right) dy \qquad \delta_2 = -\int_o^\delta \frac{W}{U_1}\, dy$$

$$\theta_{11} = \int_o^\delta \left(1 - \frac{U}{U_1}\right)\frac{U}{U_1}\, dy \qquad \theta_{12} = \int_o^\delta \left(1 - \frac{U}{U_1}\right)\frac{W}{U_1}\, dy$$

$$\theta_{21} = -\int_o^\delta \frac{UW}{U_1^2}\, dy \qquad \theta_{22} = -\int_o^\delta \frac{W^2}{U_1^2}\, dy$$

and the shape factor is defined as $H = \delta_1/\theta_{11}$. The wall friction coefficients measured are presented as a function of the unit Reynolds number U_1/ν.

TWO-DIMENSIONAL RESULTS

The two-dimensional measurements were made 9 ft downstream from the entrance of the test section and 8 in. from one wall. Two boundary-layer surveys were made at free-stream velocities of 101 and 80 ft/sec. The unit Reynolds numbers were $5.87X10^5$ 1/ft and $4.65X10^5$ 1/ft. Figure 17 gives the profiles, and Table 2 gives the data. Figure 18 gives the wall-friction coefficients obtained with Preston tubes 1 and 2. A mean line has been faired through the individual data points. Also shown are values of c_{w_1} obtained from some standard two-dimensional formulas, using the experimental values of the integral thicknesses. Values of the integral thicknesses and the shape factor obtained from the measured velocity profiles are given in Table 3, and the formulae used are listed as follows.

Schoenherr[13]

$$c_{w_1} = \frac{0.310}{\ln^2\left(2R_{\theta_{11}}\right) + 2\ln\left(2R_{\theta_{11}}\right)} \tag{1}$$

Ludwieg and Tillmann[14]

$$c_{w_1} = 0.246 \times 10^{-0.678H} R_{\theta_{11}}{}^{-0.268} \tag{2}$$

Clauser[15]

$$1/\sqrt{c_{w_1}} = 3.96 \log R_{\delta_1} + 3.04 \tag{3}$$

Squire and Young[16]

$$1/\sqrt{c_{w_1}} = 4.17 \log R_{\theta_{11}} + 2.54 \tag{4}$$

The measured and calculated values of skin friction obtained by the various methods are in substantial agreement. The worst case is a difference of approximately 2.3 percent between the mean of the Preston tube results and the Squire and Young formula.

---

[13]Landweber, L., "The Frictional Resistance of Flat Plates in Zero Pressure Gradient," Transactions of the Society of Naval Architects and Marine Engineers, Vol. 61 (1953).

[14]Ludwieg, H. and W. Tillmann, "Investigations of the Wall-Shearing Stress in Turbulent Boundary Layers," National Advisory Committee for Aeronautics, Technical Memorandum 1285 (1950); Zeitschriff für angewandte, Mathemati and Mechani, Vol. 29 (1949).

[15]Clauser, F.H., "The Turbulent Boundary Layer," Advances in Applied Mechanics, Vol.4, Academic Press, Inc., New York (1956).

[16]Squire, H.B. and A.D. Young, "The Calculation of the Profile Drag of Airfoils," ARC, Report and Memorandum 1838 (1938).

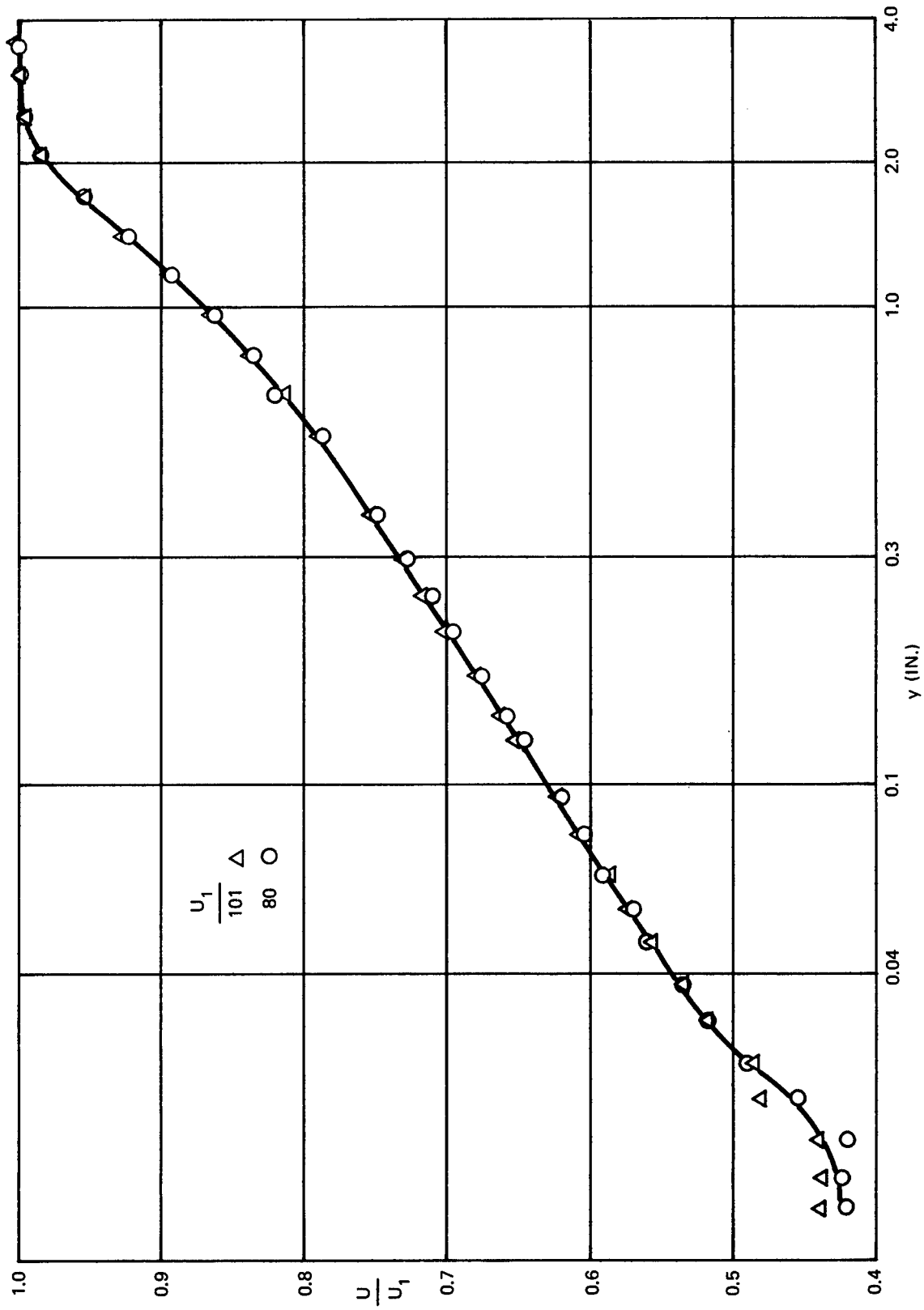

Figure 17 – Two-Dimensional, Boundary-Layer Velocity Profiles

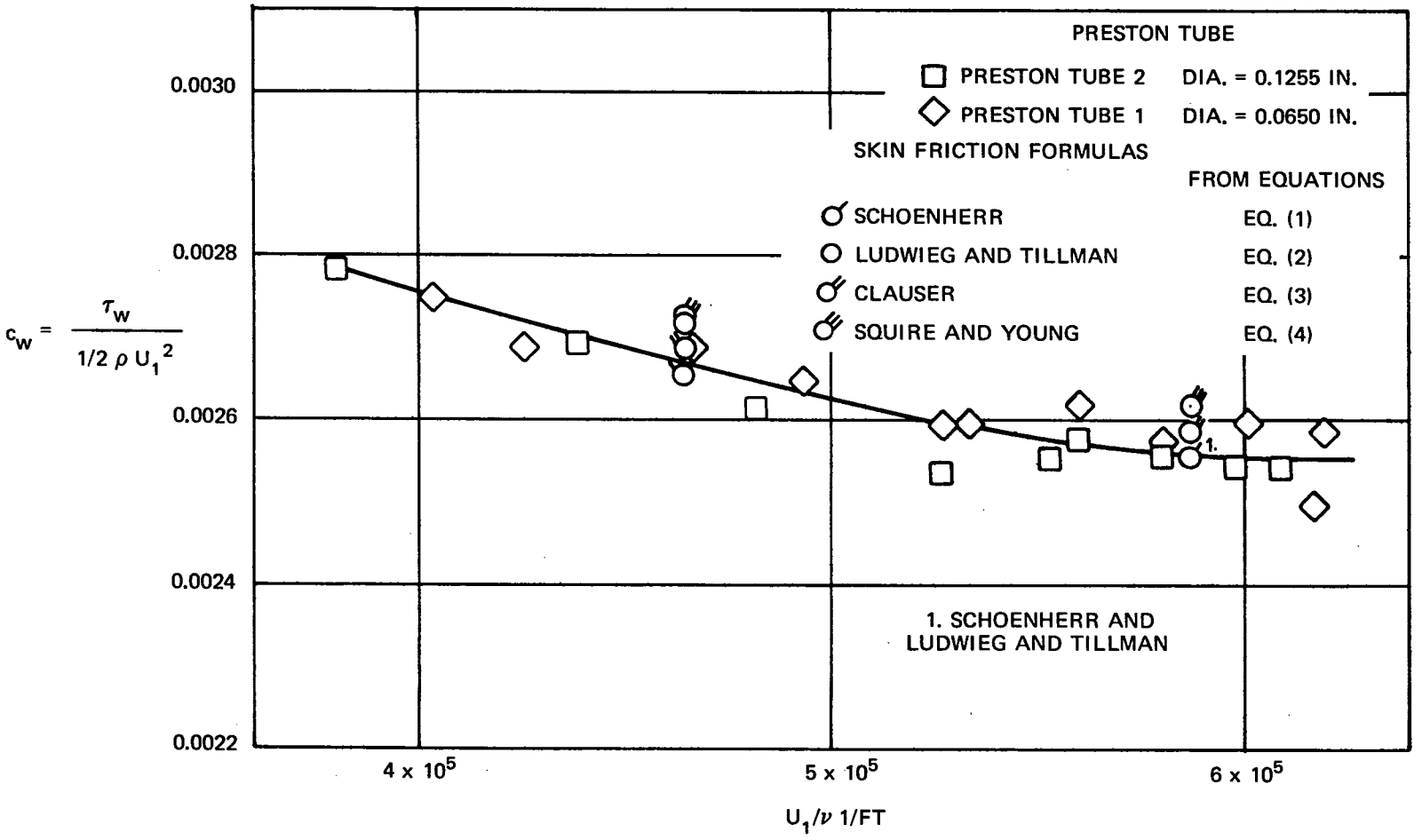

Figure 18 – Two-Dimensional, Wall-Friction Coefficient

TABLE 2 – TWO-DIMENSIONAL VELOCITY PROFILES

	U/U_1	
y in.	U_1 = 80 ft/sec	U_1 = 101 ft/sec
0.013	0.424	0.441
0.015	0.425	0.441
0.018	0.423	0.443
0.022	0.456	0.483
0.026	0.491	0.489
0.032	0.518	0.520
0.038	0.538	0.539
0.047	0.561	0.560
0.055	0.571	0.576
0.065	0.591	0.589
0.079	0.606	0.609
0.095	0.622	0.625
0.125	0.647	0.655
0.140	0.660	0.665
0.170	0.677	0.682
0.210	0.697	0.702
0.250	0.712	0.719
0.300	0.729	0.735
0.370	0.749	0.756
0.540	0.788	0.793
0.660	0.822	0.816
0.800	0.837	0.840
0.970	0.864	0.866
1.180	0.894	0.896
1.420	0.924	0.931
1.720	0.956	0.956
2.100	0.984	0.985
2.550	0.998	0.997
3.100	1.000	0.999
3.660	1.000	1.000

TABLE 3 – TWO-DIMENSIONAL BOUNDARY-LAYER PROPERTIES

U_1 ft/sec	δ_1 in.	θ_{11} in.	Shape Factor
80	0.322	0.245	1.313
101	0.317	0.241	1.317

THREE-DIMENSIONAL RESULTS

For these preliminary experiments, it was decided to use an S-shaped tunnel with the curvature close to the limit allowed by the wall flexibility. In addition, the distance between the walls was gradually increased, creating a moderate adverse pressure gradient along the tunnel. It was felt that these conditions would produce a typical three-dimensional, shiplike boundary layer in the tunnel. The shape of the tunnel along with the measured pressure gradient is given in Figure 19, where p_o is the pressure at the test section entrance, and p_1 is the pressure along the tunnel. Also shown are positions 1 and 2 at which the boundary-layer surveys were made.

The results of the three-dimensional tests are presented in Figures 20 through 24. Figure 20 is a semilog plot of the velocity-vector profiles, while the range of β with y is presented in Figure 21. The data presented in these plots are given in Table 4. Figures 22 and 23 give U and W component profiles at Positions 1 and 2. The Preston tube results are presented in Figure 24, and the values of β_o, δ, integrated properties of the profiles; the shape factor, and unit Reynolds number are given in Table 5.

Owing to limited data, no analysis of the cross flow-velocity profiles has been attempted. However, the experimental results have been compared with the Mager cross flow profile[17]

$$\frac{W}{U} = \frac{U}{U_1}\left(1 - y/\delta\right)^2 \tan \beta_o \tag{5}$$

where U/U_1 is given by the power-law relation

$$\frac{U}{U_1} = \left(\frac{y}{\delta}\right)^{\frac{H-1}{2}} \tag{6}$$

The values of δ, β_o, and H used in the previous equations have been obtained from the experimental data. The use of Equations (5) and (6), when valid, provides a simple means of obtaining cross flow, momentum-thickness formulas in terms of overall boundary-layer parameters such as H and δ. Equation (6) is not to be taken as an accurate formula for the streamwise flow. Equations (5) and (6) are compared with the data from Positions 1 and 2 in Figures 23 and 24. Equation (6) gives a reasonably close approximation to the experimental values of U/U_1 and when used in Equation (5) gives cross flow results substantially the same as those obtained using the experimental values of U/U_1. At Position 1, with a maximum skew of 10.5 deg, the experimental plot of the cross flow agrees fairly well with the Mager profile. At Position 2, with a maximum skew of 6 deg, there is a difference of approximately 50 percent between the Mager profile and the experimental values.

[17]Mager, A., "Generalization of Boundary Layer Momentum Integral Equations to Three-Dimensional Flows Including Those of Rotating Systems," National Advisory Committee for Aeronautics, Report 1067 (1952).

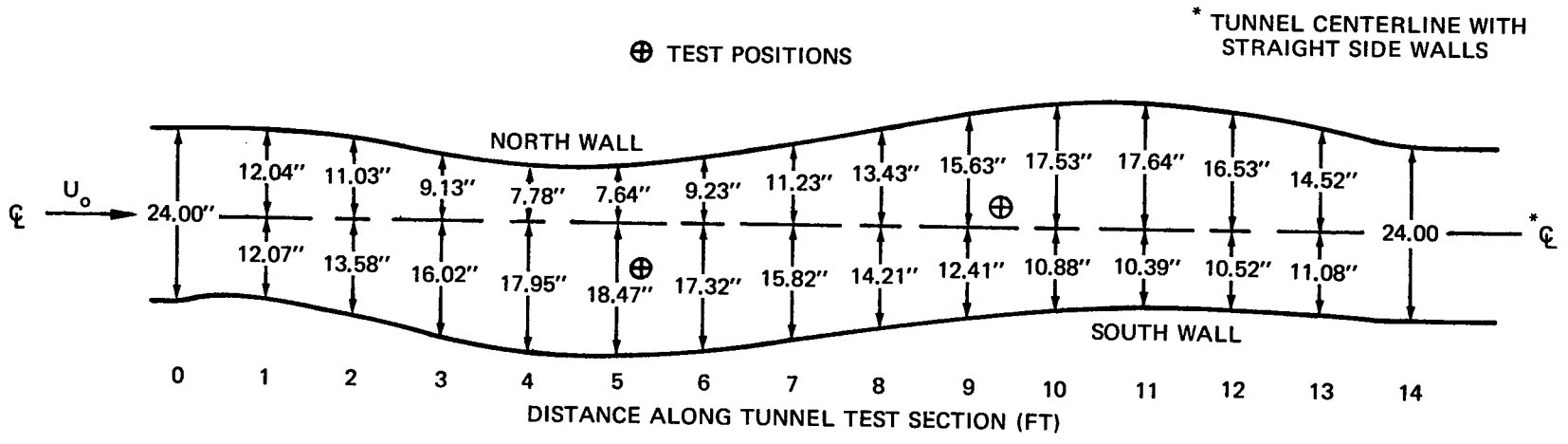

Figure 19a – Tunnel Wall Shape

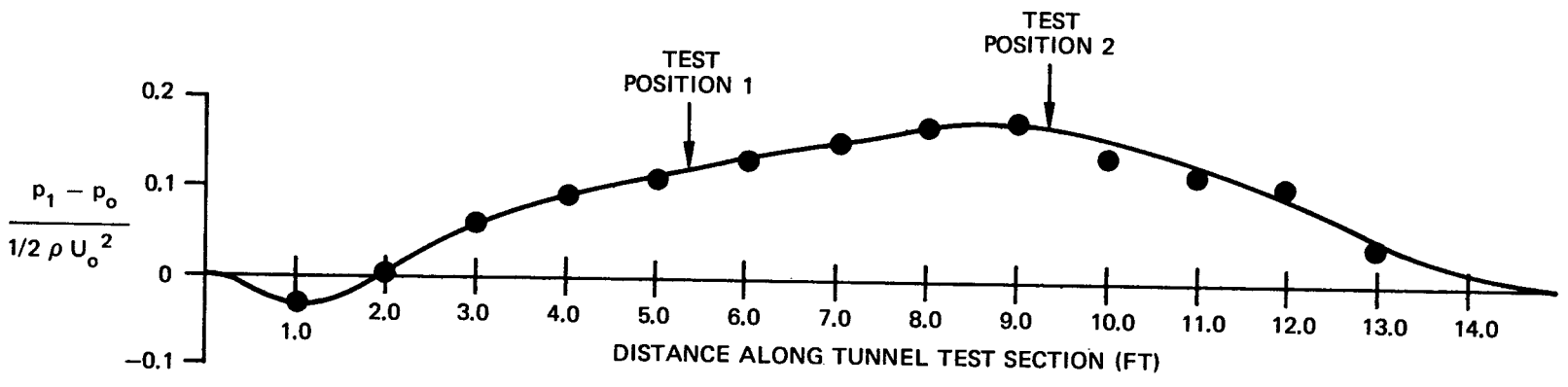

Figure 19b – Tunnel Pressure Gradient

Figure 19 – Tunnel Geometry and Pressure Gradient

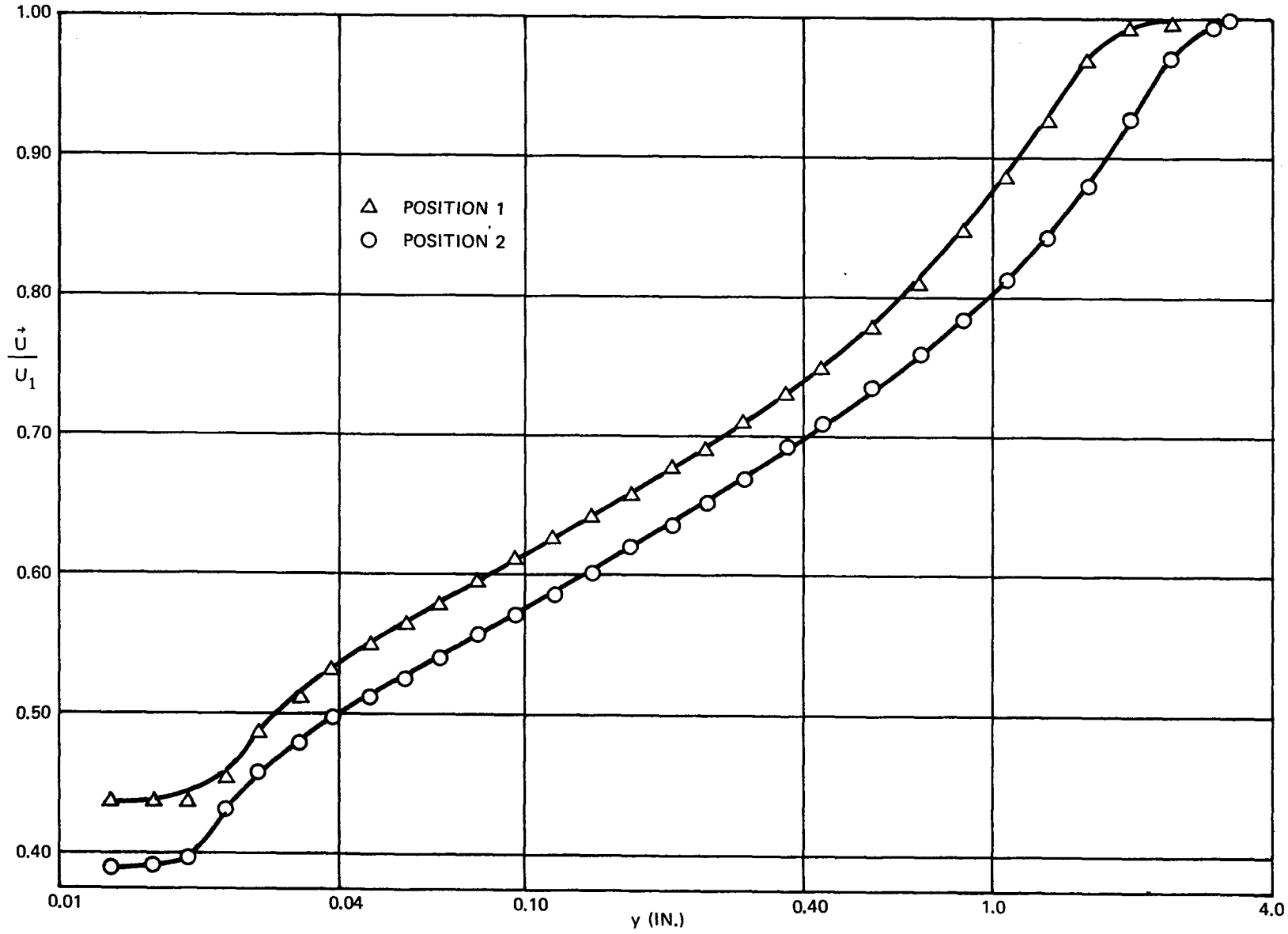

Figure 20 – Three-Dimensional, Boundary-Layer, Velocity Profiles

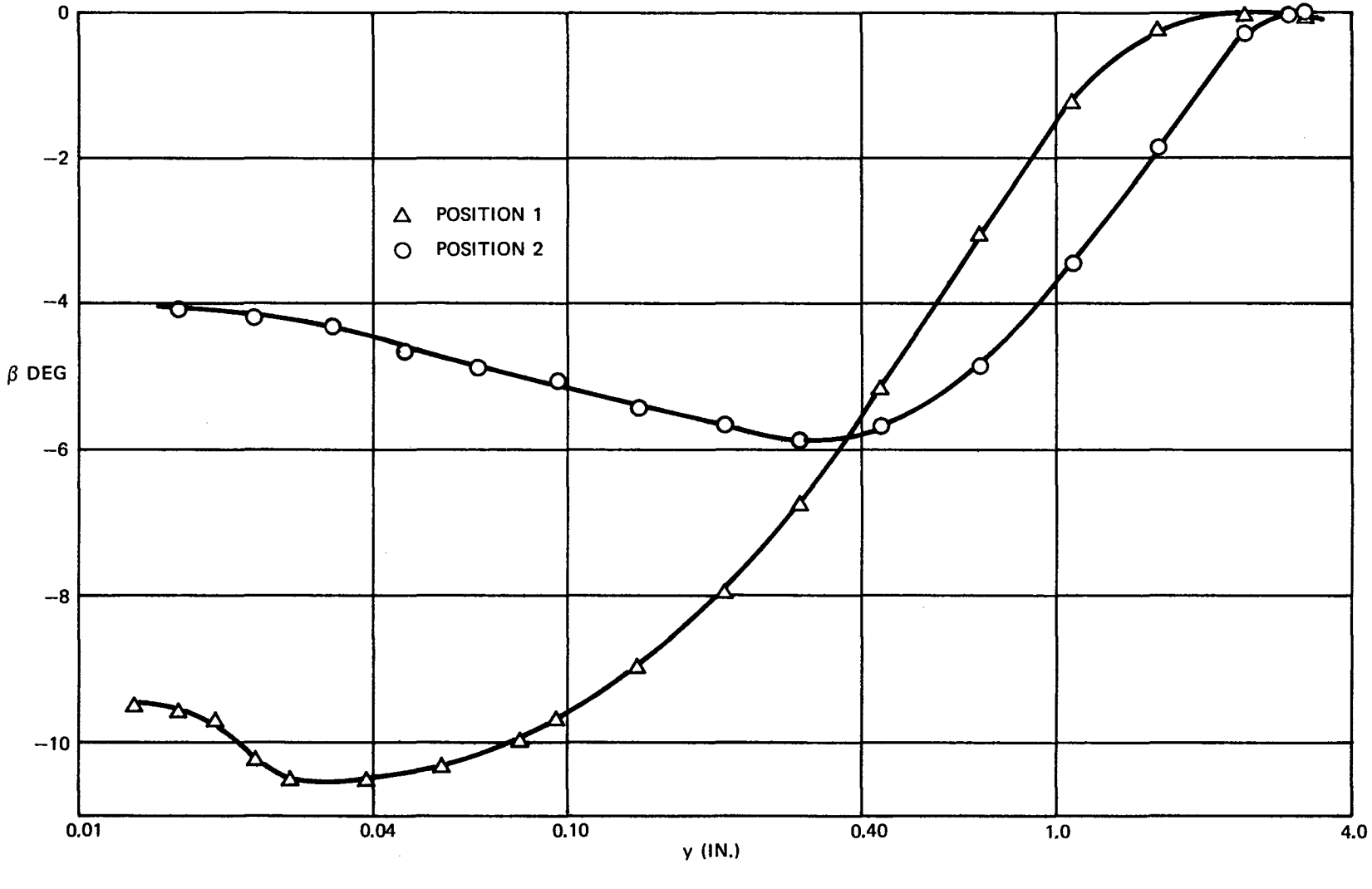

Figure 21 – Boundary-Layer Velocity-Vector Direction

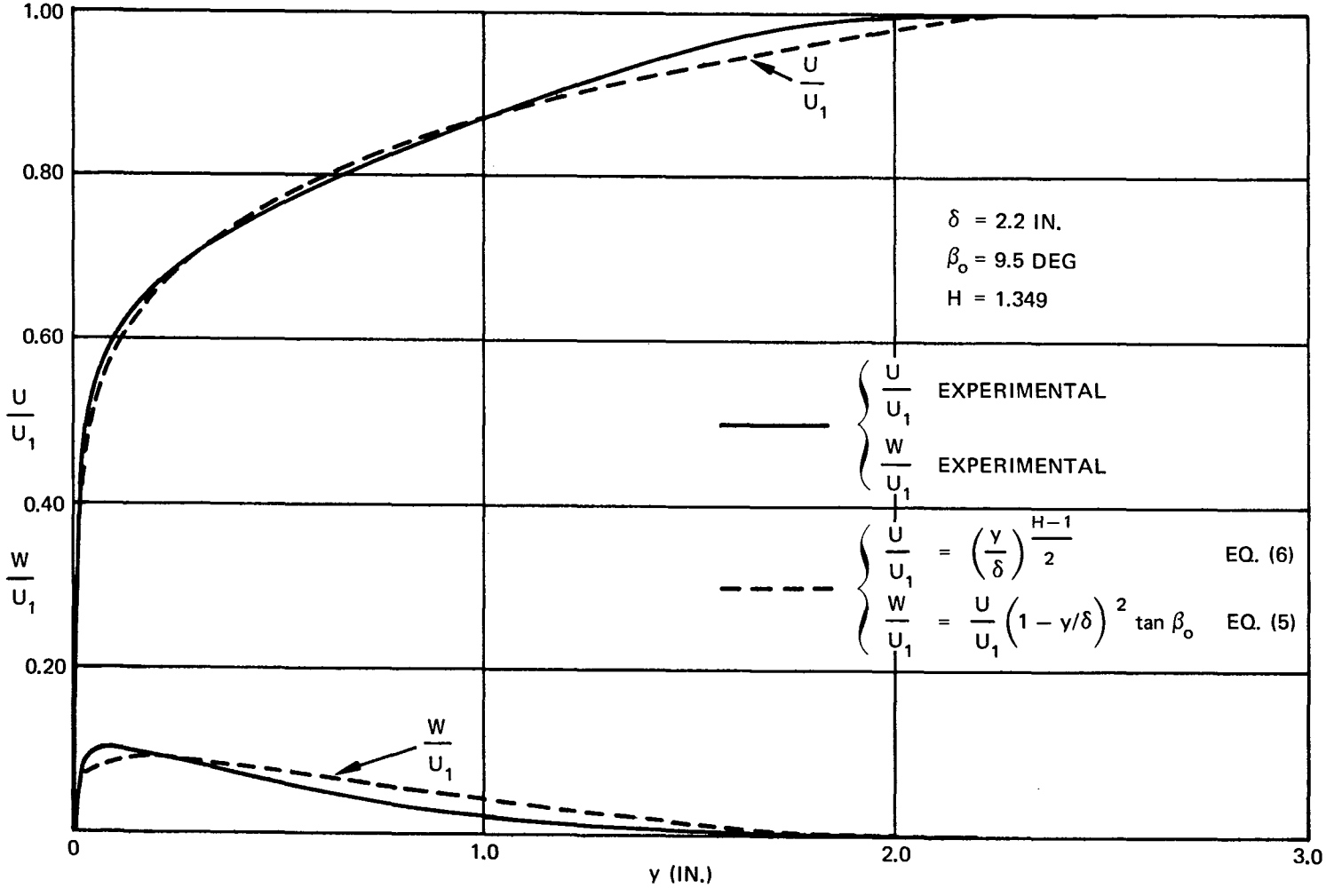

Figure 22 – Boundary-Layer, Velocity Components at Position 1

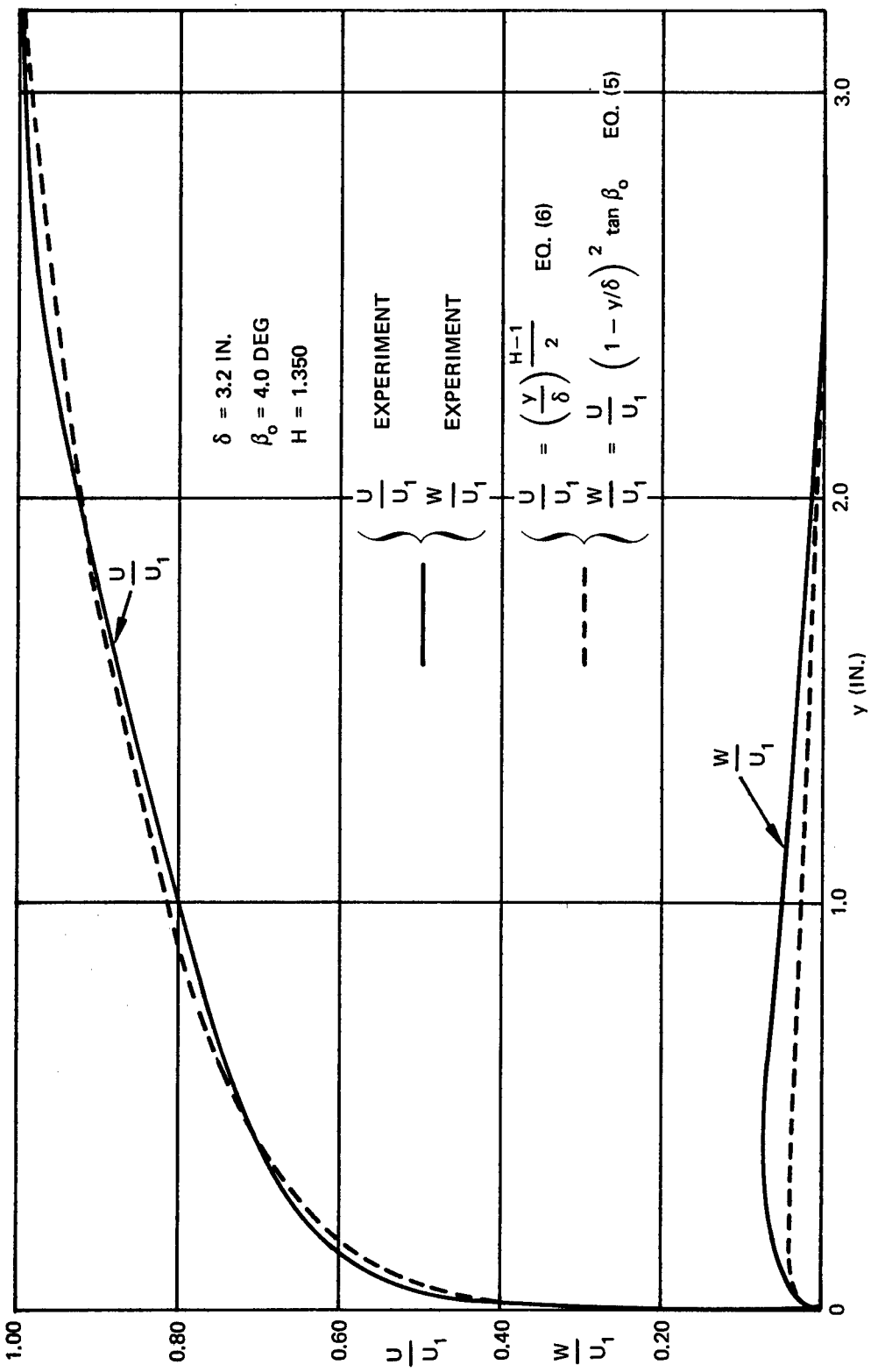

Figure 23 — Boundary-Layer, Velocity Components at Position 2

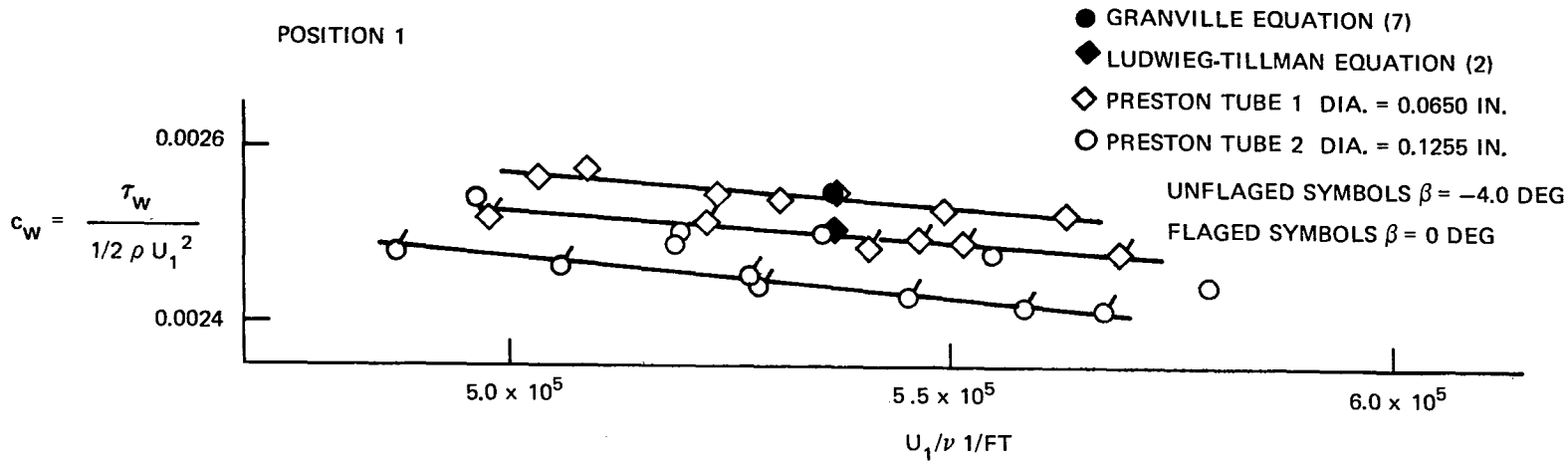

Figure 24a

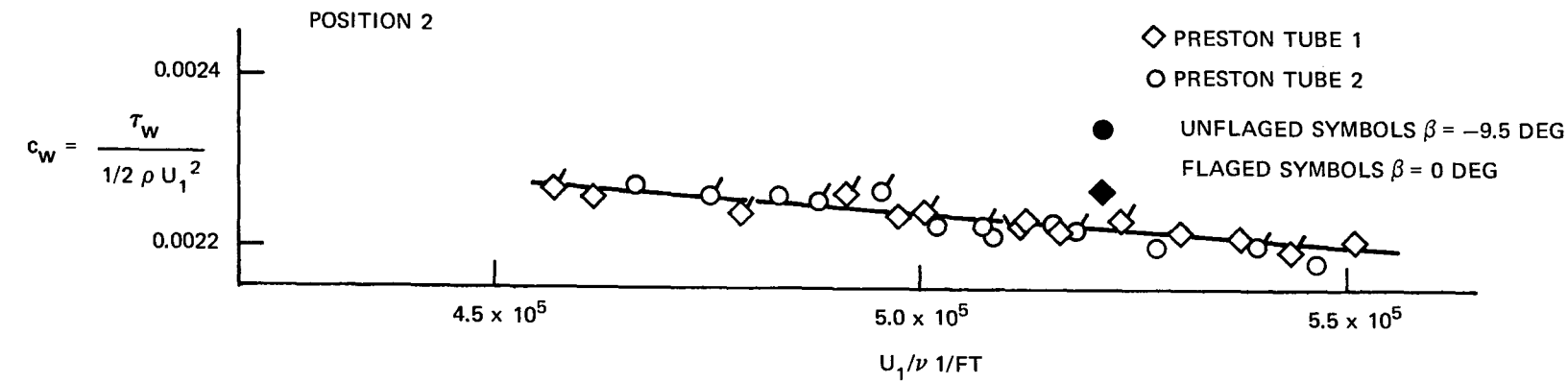

Figure 24b

Figure 24 — Three-Dimensional, Preston Tube Results

TABLE 4 – THREE-DIMENSIONAL VELOCITY PROFILES

	Position 1		Position 2	
y in.	$\vec{U}/U_1$ ft/sec	β deg	$\vec{U}/U_1$ ft/sec	β deg
0.013	0.439	- 9.48	0.390	–
0.016	0.439	- 9.56	0.392	-4.07
0.019	0.437	- 9.68	0.397	–
0.023	0.456	-10.21	0.433	-4.14
0.027	0.488	-10.48	0.459	–
0.033	0.515	–	0.481	-4.29
0.039	0.534	-10.49	0.498	–
0.047	0.551	–	0.514	-4.64
0.056	0.566	-10.31	0.526	–
0.066	0.579	–	0.541	-4.85
0.080	0.595	- 9.93	0.558	–
0.096	0.611	- 9.70	0.571	-5.06
0.116	0.627	–	0.587	–
0.141	0.643	- 8.94	0.603	-5.39
0.171	0.660	–	0.621	–
0.211	0.679	- 7.94	0.637	-5.64
0.251	0.691	–	0.654	–
0.301	0.711	- 6.71	0.671	-5.85
0.371	0.732	–	0.694	–
0.441	0.750	5.14	0.710	-5.64
0.561	0.780	–	0.735	–
0.701	0.812	- 3.04	0.760	-4.85
0.871	0.848	–	0.784	–
1.081	0.887	- 1.21	0.813	-3.43
1.321	0.928	–	0.844	–
1.621	0.971	- 0.22	0.880	-1.84
2.001	0.995	–	0.928	–
2.451	0.999	0	0.973	-0.31
3.001	1.000	–	0.996	0
3.241	1.000	- 0.05	1.000	0

The results of the Preston tube measurements at Position 1 are given in Figure 24a. The friction was measured with the Preston tubes aligned in the inviscid streamline and β_o directions. The results from both tubes showed a variation in the measured values of c_w, values in the inviscid streamline direction being approximately 2 percent less than the values in the β_o, -9.5 deg direction. There was also a difference of approximately 2 percent in the values of c_w measured by the two Preston tubes. This was true in both the free-stream and β_o directions, indicating a possible effect of cross flow skew across a Preston tube diameter on the tube readings.

The previously described measurements were repeated at Position 2, and the results are shown in Figure 24b. In this case there was no discernable difference in the measured c_w for the four sets of data; however, the difference between free-stream direction and β_o was much smaller, 4.0 deg, and the boundary-layer skew was much less.

TABLE 5 – THREE-DIMENSIONAL BOUNDARY-LAYER PROPERTIES

	Position 1	Position 2
β_o	9.5 deg	4.0 deg
δ	2.2 in.	3.2 in.
δ_1	0.3133 in.	0.4709 in.
δ_2	-0.0710 in.	-0.0993 in.
θ_{11}	0.2322 in.	0.3487 in.
θ_{12}	0.0194 in.	0.0231 in.
θ_{21}	-0.0524 in.	-0.0777 in.
θ_{22}	-0.0047 in.	-0.0051 in.
H	1.349	1.350
U_1/ν	5.37×10^5 1/ft	5.21×10^5 1/ft

Also shown in Figure 24 are values of c_{w_1}, computed from the integrated properties of the boundary-layer profiles. Two two-dimensional, skin-friction laws for pressure gradients have been used; Ludwieg and Tillmann, Equation (2), and Granville[18]:

$$c_{w_1} = \frac{0.0292 \left(\frac{Q}{Q_o}\right)^{\frac{4}{H_o + 1}}}{\log\left(2R_{\theta_{11}}\right)\left[\frac{1}{2}\log\left(2R_{\theta_{11}}\right) + 0.4343\right]}$$

$$H_o = \frac{1.475}{\log R_{\theta_{11}}} + 0.9698 \qquad (7)$$

$$Q = 0.9058 - 1.818 \log H$$

$$Q_o = 0.9058 - 1.818 \log H_o$$

Both of these formulas give values of c_{w_1} that are higher than the Preston tube results at Position 2. The Ludwieg and Tillmann formula gives values closer to the measured values than the Granville formula. At Position 1 the agreement is closer. The Ludwieg and Tillmann formula agrees well with the 0.065-in. diameter Preston tube results, while the Granville formula gives slightly higher results. However, the discrepancy in the Preston tube readings at this position prevents definite conclusions being drawn.

[18]Granville, P.S., "Integral Methods for Turbulent Boundary Layers in Pressure Gradients" NSRDC Report 3308 (1970).

DISCUSSION

The main purpose of the program described here has been to produce and determine the characteristics of three-dimensional turbulent boundary layers similar to ship boundary layers. Two principle features of a ship boundary layer are the cross flow produced by transverse pressure gradients and the effect of longitudinal pressure gradients. The only information about ship cross flow available to the author may be found in References 19 and 20. In Reference 19 the value of β_o was computed along a ship streamline where typical maximum and minimum cross flow angles occurred. The ship used as a model was the LUCY ASHTON, and the method of Reference 1 was used for the calculations. The author concludes that the maximum value of β_o would be less than 8 deg.

In Reference 20 the flow around the Mariner-Class ship USS COMPASS ISLAND was observed by photographing tufts attached to the hull. Some of the tufts were attached directly on the hull; others were fastened to pins and were located an inch away from the hull. Although this method was too crude to give accurate quantitative measurements, careful observations of the alignments of the two sets of tufts indicated only small cross flow in the boundary layer. Thus the results agreed qualitatively with those computed in Reference 19, and the results at Position 1 of β_o = 9.5 deg have shown that boundary layers with similar cross flow can be produced in the tunnel.

Computed longitudinal pressure distributions for LUCY ASHTON are also given in Reference 19. These pressure distributions were used to compute the necessary tunnel-wall separation to obtain similar pressure distributions along the tunnel. These separations are well within the tunnel capabilities. Since LUCY ASHTON and COMPASS ISLAND are ships of moderate block coefficients, it can be concluded that three-dimensional boundary layers with cross flow and longitudinal pressure gradients similar to those on ships of small and moderate block coefficients can be reproduced in the wind tunnel.

The cause of the discrepancy in shear measurements at Position 1 is not known. However it is believed that the effect is real, since it has appeared in independent measurements in the β_o and inviscid stream directions. A similar effect was observed by Prahlad.[21] He measured β_o in flows of widely varying β_o, o to 57 deg, using six different Preston tubes with diameters ranging from 0.0585 to 0.0195 in. He found that for some flows, such as, β_o = 27.5, 53.5, and 56.5 deg, the four larger Preston tubes gave lower values of c_w than the two smaller tubes. For other flows, such as, β_o = 26.5, 140, 11.0, 4.5, and 0 deg, all tubes gave the same value of c_w. When disagreement was present, Prahlad attributed it to the existence of a favorable pressure gradient and showed that the boundary layer profile departed from the two-dimensional law of the wall. In the present case, the data at Position 1 were obtained in an adverse pressure gradient and, as can be seen from Figure 25, agreed fairly well with the law of the wall. Also, both Preston tubes were well within the law of the wall region for all tests. Result at Position 1 indicates that Preston tubes should be used with caution when measuring skin friction in three-dimensional boundary layers.

---

[19]von Kerczek, C.W., "Calculation of the Turbulent Boundary Layer of a Ship Hull at Zero Froude Number," Journal of Ship Research, Vol. 17, No. 2 (1973).

[20]Newman, J.N., "Some Hydrodynamic Aspects of Ship Maneuverability," Proceedings of the Sixth Symposium of Naval Hydrodynamics (1966).

[21]Prahlad, T.S., "Wall Similarity in Three-Dimensional Turbulent Boundary Layers," American Institute of Aeronautics and Astronautics Journal, Vol. 6, p. 1772, (1968).

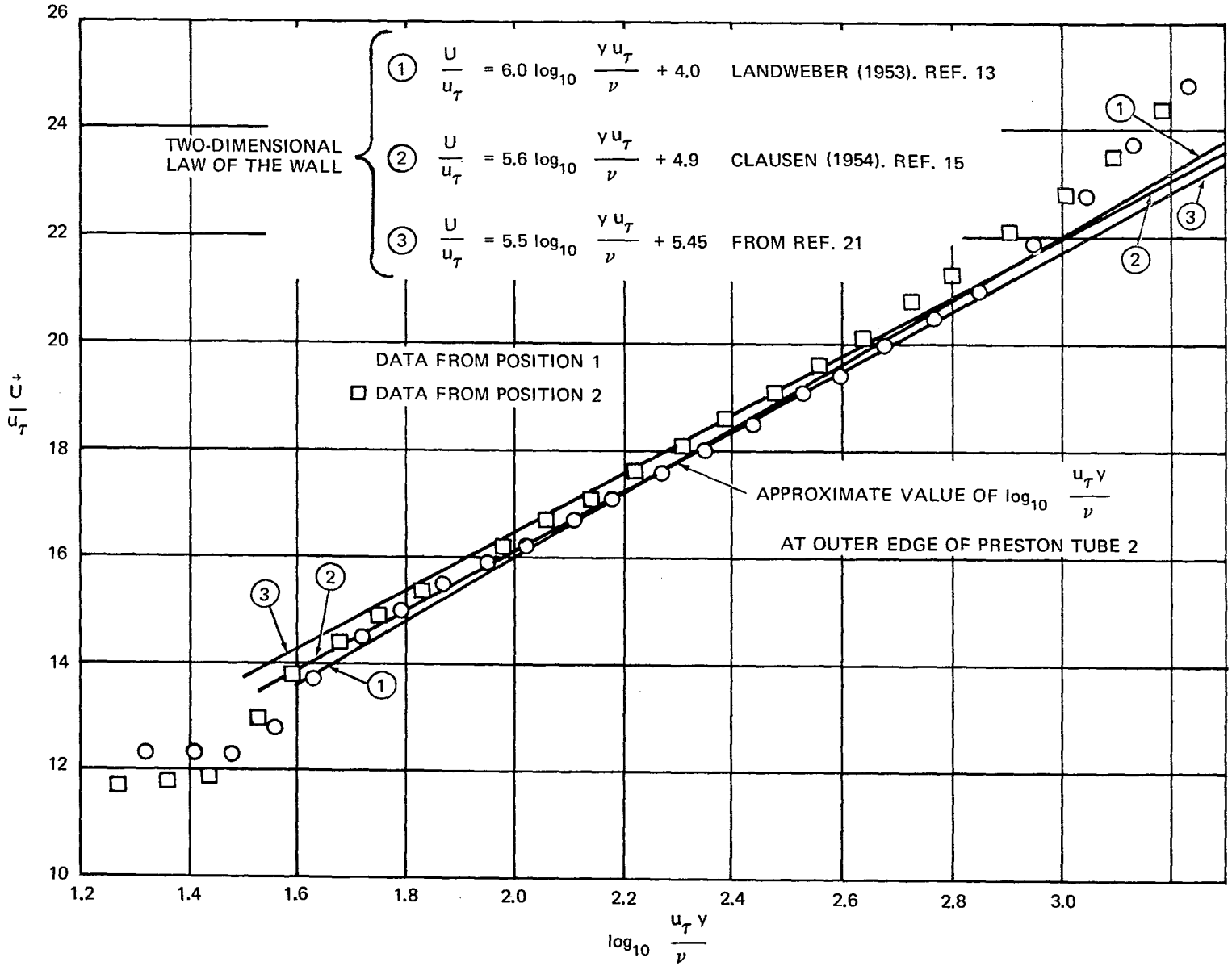

Figure 25 – Comparison of Data from Positions 1 and 2 with Two-Dimensional Law of the Wall

Two important items that were to be checked in the test program were the validity of the Mager cross flow-profile assumption[17] and of the two-dimensional velocity similarity law skin-friction formulas for obtaining the inviscid streamline component of skin friction. As can be seen in Figures 22 and 23, the Mager cross flow profile provides a poor fit to the experimental cross flow profiles. Surprisingly, it is worse for the profile with the smaller cross flow parameter β.

In applying the small cross flow approximation – i.e., assuming that θ_{12} and θ_{22} and their derivatives are small compared to θ_{11}, which allows simplification of the momentum integral equations[3] for three-dimensional boundary layers – and the Mager cross flow profiles to boundary-layer calculation methods, it is important to assess the accuracy of the prediction of θ_{21}. By using the Mager cross flow and the power-law profiles, Equations (5) and (6), the expression for θ_{21} becomes

$$\theta_{21} = -\frac{2\,\delta \tan \beta_o}{H\,(H+1)\,(H+2)} \tag{8}$$

Using measured values of δ, β_o, and H – e.g., at Position 1, δ = 2.2 in., β_o = 9.5 deg, and H = 1.349, while at Position 2, δ = 3.2 in., β_o = 4 deg, and H = 1.350 – Equation (8) gives at Position 1, θ_{21} = -0.069 in., and at Position 2, θ_{21} = -0.041 in. Comparing these values to the experimental values of θ_{21} (Table 3) shows the discrepancy to be greater than 20 percent, reflecting errors in the fit of the Mager profile to the experimental cross flow profiles.

From the definition of the boundary-layer thicknesses, the following identity can be obtained

$$\theta_{21} = \theta_{12} + \delta_2 \tag{9}$$

and the experimental values of θ_{21}, θ_{12}, and δ_2 in Table 3 satisfy this relation with less than a 2-percent discrepancy, giving a consistency check of the experimental results. Further, all the cross flow thicknesses are small compared to δ_1 and θ_{11}. This shows that for three-dimensional boundary layers similar to those investigated here the small cross flow approximation for the streamline component of the boundary-layer calculation may be a fairly good approximation, provided that the derivative of the cross flow terms also remain small. However, the Mager profile is not a good representation of the cross flow, and an approximate calculation of the cross flow based on it would not be adequate.

A second consideration in these experiments was to see whether two-dimensional, skin-friction laws, when applied to the streamwise component of the flow in the boundary layer, would be adequate with a small cross flow. Figure 24 shows that the Ludwieg and Tillmann formula agrees reasonably well with the data; however, the Granville formula overpredicts the value of c_{w_1}. The data available are too sparse to make a meaningful assessment of the validity of the two formulas; however, it is evident that the Granville formula is suspect.

CONCLUSIONS

1. The tunnel is a suitable facility for studying three-dimensional turbulent boundary layers similar to those occurring on ships having small or moderate block coefficients.
2. The Mager cross flow profile provides a poor fit to the data obtained at the two positions, indicating that this profile is not always a good representation of the cross flow in a three-dimensional boundary layer.
3. All the cross flow thicknesses were small, indicating that the small cross flow approximation in calculation methods might be useful for cross flows of the magnitude studied in these tests.
4. The Preston tube results agreed well with results computed with the Ludwieg and Tillmann two-dimensional skin-friction law. The Granville formula gave results 2 and 5 percent higher than the Preston tube results.
5. Results at Position 1 indicated that the variation in cross flow in the log region of the boundary layer could affect Preston tube readings. Therefore, Preston tubes should be used with caution in three-dimensional boundary layers.

ACKNOWLEDGMENTS

The author is grateful to Dr. Christian W. von Kerczek for his advice during planning of the experiment and his critical review of this report.

REFERENCES

1. Cumpsty, N.A. and M.R. Head, "The Calculation of Three-Dimensional Turbulent Boundary Layers, Part 1: Flow Over the Rear of an Infinite Swept Wing," The Aeronautical Quarterly, Vol. 18 (1967).

2. Bradshaw, P., "The Calculation of Three-Dimensional Turbulent Boundary Layers," Journal of Fluid Mechanics, Vol. 46, Part 3 (1971).

3. Nash, John T. and V.C. Patel, "Three-Dimensional Turbulent Boundary Layers," SEC Technical Books, Scientific and Business Consultants, Inc., Atlanta, Ga. (1972).

4. Johnston, J.P., "Measurements in a Three-Dimensional Turbulent Boundary Layer Induced by a Swept, Forward-Facing Step," Journal of Fluid Mechanics, Vol. 42, Part 4, pp. 823-844 (1970).

5. East, L.T. and R.P. Hoxey, "Low Speed Three-Dimensional Turbulent Boundary Layer Data," Parts 1 and 2, Aeronautical Research Council, R and M 3653 (1969).

6. Hornung, H.G. and P.N. Joubert, "The Mean Velocity Profile in Three-Dimensional Turbulent Boundary Layers," Journal of Fluid Mechanics, Vol. 5, Part 3 (1963).

7. Grunschwitz, E., "Turbulente Reigungsschichten mit Sekundarstromoung," Ingeniuer-Archiv, Vol. VI, (1935).

8. Francis, G.P. and F.J. Pierce, "An Experimental Study of Skewed Turbulent Boundary Layers in Low Speed Flows," Journal of Basic Engineering, Transactions American Society of Mechanical Engineers, Series D, Vol. 89, No. 3, pp. 597-607 (1967).

9. Johnston, J.P., "On the Three-Dimensional Turbulent Boundary Layer Generated by Secondary Flow," Journal of Basic Engineering, Transactions American Society of Mechanical Engineers, Series D, Vol. 82, pp. 233-248 (1960).

10. Scottron, V.E. and D.A. Shaffer, "The Low Turbulence Wind Tunnel," David Taylor Model Basin, Report 2116 (Dec 1965).

11. Smith, A.M.O. and J.S. Murphy, "Micromanometer for Measuring Boundary Layer Profiles," The Review of Scientific Instruments, Vol. 26, No. 8 (Aug 1955).

12. Head, M.R. and V.V. Ram, "Simplified Presentation of Preston Tube Calibration," The Aeronautical Quarterly (Aug 1971).

13. Landweber, L., "The Frictional Resistance of Flat Plates in Zero Pressure Gradient," Transactions of the Society of Naval Architects and Marine Engineers, Vol. 61 (1953).

14. Ludwieg, H. and W. Tillmann, "Investigations of the Wall-Shearing Stress in Turbulent Boundary Layers," National Advisory Committee for Aeronautics, Technical Memorandum 1285 (1950); Zeitschriff für angewandte, Mathemati and Mechani, Vol. 29 (1949).

15. Clauser, F.H., "The Turbulent Boundary Layer," Advances in Applied Mechanics, Vol. 4, Academic Press, Inc., New York (1956).

REFERENCES (Continued)

16. Squire, H.B. and A.D. Young, "The Calculation of the Profile Drag of Airfoils," ARC, Report and Memorandum 1838 (1938).

17. Mager, A., "Generalization of Boundary Layer Momentum Integral Equations to Three-Dimensional Flows Including Those of Rotating Systems," National Advisory Committee for Aeronautics, Report 1067 (1952).

18. Granville, P.S., "Integral Methods for Turbulent Boundary Layers in Pressure Gradients" NSRDC Report 3308 (1970).

19. von Kerczek, C.W., "Calculation of the Turbulent Boundary Layer of a Ship Hull at Zero Froude Number," Journal of Ship Research, Vol. 17, No. 2 (1973).

20. Newman, J.N., "Some Hydrodynamic Aspects of Ship Maneuverability," Proceedings of the Sixth Symposium of Naval Hydrodynamics (1966).

21. Prahlad, T.S., "Wall Similarity in Three-Dimensional Turbulent Boundary Layers," American Institute of Aeronautics and Astronautics Journal, Vol. 6, p. 1772, (1968).

INITIAL DISTRIBUTION

Copies	
1	Army Air Mobil R&D Lab
4	CHONR 3 Code 438 1 Code 460
1	USNA
1	NAVPGSCOL
1	NROTC & NAVADMINU, MIT
1	NAVWARCOL
1	NRL
7	NAVSHIPSYSCOM 2 SHIPS 2052 1 SHIPS 031 1 SHIPS 03411 1 SHIPS 03412 2 PMS-395
1	NAVAIRSYSCOM
3	NAVORDSYSCOM 1 ORD 035 2 ORD 054131
1	NELC
3	NAVUSEACEN SAN DIEGO 1 A. Fabula 1 T. Lang
3	NAVUSEACEN PASADENA 1 J. Hoyt 1 J. Waugh
1	NAVWPNSCEN
6	NOL 1 V. Dawson 1 A. May 1 A. Seigel 1 N. Tetervin 1 R. Wilson
4	NPTLAB NUSC 1 J. Brady 1 P. Gibson 1 R. Nadolink
1	NLONLAB NUSC
4	NAVSEC 1 SEC 6110.01 1 SEC 6114 1 SEC 6114D 1 SEC 6115
2	AFOSR 1 518, M. Rogers

Copies	
1	AFWL WLDE-3, CAPT Young
12	DDC
1	MARAD Ships Res & Dev
1	HQS NASA A. Gessow
4	NASA Ames Res Cen 1 G. Deiwert, MS 229-4 1 J. Murphy, MS 227-8 1 W. Rose, MS 227-8 1 M. Rubesin, MS 230-1
1	NASA Langley Res Cen I. Beckwith, MS 161
1	National Science Foundation Engr Sci Div
2	BUSTAND 1 Kuhn, Hydr Lab 1 P. Klebanoff
1	U Bridgeport E. Uram, Grad Scol Engr
3	U California, Berkeley 1 G. Corcos Dept Mech Engr 2 Dept NAME
1	U California, Los Angeles A. Mills, Dept Engr
1	U California, Santa Cruz F. Caluser
3	Cal Inst of Technol 1 Hydro Lab, A. Acosta 2 Karman Lab 1 D. Coles 1 H. Liepmann
4	Catholic U 1 M. Casarella 1 P. Chang 1 Kelnhofer
2	Colorado State U 1 Cermack Fluid Dyn & Diffusion Lab 1 V. Sandborn
1	U Connecticut V. Scottron
2	Harvard U 1 H. Emmons 1 R. Kronauer Engr & Appl Phys

Copies	
1	Illinois Inst of Technol M. Morkovin Aero & Mech Engr
1	Iowa Inst of Hydr Res L. Landweber
1	Johns Hopkins U L. Kovasznay, Mech
5	MIT 1 M. Escudier, Mech Engr 4 Dept Ocean Engr 1 M. Abkowitz 1 J. Newman 1 P. Mandel
2	U Michigan 1 W. Willmarth Dept Aero Engr 1 Dept NAME
1	U Minnesota St. Anthony Falls Hydr Lab
1	Notre Dame V. Nee, Mech Engr
5	Penn State U 4 App Res Lab 1 W. George 1 R. Henderson 1 J. Lumley 1 Aero Engr Dept H. Tennekes
2	Princeton U 1 H. Herring Scol Engr & Appl Sci 1 G. Mellor Dept Aero & Mech Sci
4	Purdue U 1 D. Abbot, Fluid Mech Lab 1 G. Deboy, Dept Mech Engr 1 V. Forsnes, Dept Mech Engr 1 V. Goldschmidt, Dept Mech Engr
1	U Rhode Island Frank White, Dept Mech Engr
4	Stanford U 1 Dept Civ Engr E. Hsu 3 Dept Mech Engr 1 J. Johnston 1 S. Kline 1 W. Reynolds
1	Tuskegee Inst E. Hirst, Dept Mech Engr
1	Virginia Poly Inst & State U H. Moses, Dept Mech Engr

Copies	
1	Webb Inst
2	Worcester Poly Inst Alden Res Lab 1 L. Hooper 1 L. Neale
1	SNAME
1	Aerojet-General J. Levy, Hydro Dept
1	Aero Res Assoc of Princeton C. Donaldson
2	Aerotherm 1 L. Anderson 1 R. Kendall
1	Boeing Company Commercial Airplane Group T. Reyhner c/o Bert Welliver
1	Esso Math & Systems R. Bernicker
1	Gen Elect Co Cincinnati J. Keith, H-45
1	Gen Motors Technical Cen G. Sovran, Engr Devel Dept
3	Hydronautics 1 M. Tulin 1 B. Silverstein
1	LTV Res Cen C.S. Wells
2	Lockheed Aircraft Corp Lockheed-Georgia Co Aero Sci Lab 1 J. Cornish 1 J. Nash
1	Martin-Marietta Corp Aero HQS J. Sternberg
1	McDonnell Douglas Corp Douglas Aircraft Co T. Cebeci
1	Nielsen Engr & Res Co J.N. Nielsen
1	North Amer Rockwell Corp Ocean Sys Op E. van Driest
1	Northrop Corp I. Alber
1	Oceanics Inc A. Lehman

Copies

1 United Aircraft Corp
Pratt & Whitney Aircraft
P. Goldberg

1 United Aircraft Corp
Res Cen, Fluid Dyn Lab
H. McDonald

1 Westinghouse Elec Corp
Underseas Div, Ocean Res &
Engr Lab
M. Macovsky

CENTER DISTRIBUTION

1	012	R. Allen
1	15	W. Cummins
1	1502	G. Stuntz
1	1504	V. Monacella
1	152	R. Wermter
1	1524	C. Wilson
1	154	W. Morgan
1	1541	P. Granville
1	1552	J. McCarthy
1	1556	D. Cieslowski
1	156	J. Hadler
1	165	R. Furey
1	165	G. Pick
1	167	S. De los Santos
1	1802.2	F. Frenkiel
1	1802.3	H. Lugt
1	1843	J. Schot

*U.S. GOVERNMENT PRINTING OFFICE:1973 542-166/Z-108 1-3

UNCLASSIFIED

Security Classification

DOCUMENT CONTROL DATA - R & D

(Security classification of title, body of abstract and indexing annotation must be entered when the overall report is classified)

1. ORIGINATING ACTIVITY *(Corporate author)*

Naval Ship Research and Development Center
Bethesda, Maryland 20034

2a. REPORT SECURITY CLASSIFICATION

Unclassified

2b. GROUP

3. REPORT TITLE

WALL SHEAR STRESS AND MEAN-VELOCITY MEASUREMENTS IN A THREE-DIMENSIONAL TURBULENT BOUNDARY LAYER

4. DESCRIPTIVE NOTES *(Type of report and inclusive dates)*

5. AUTHOR(S) *(First name, middle initial, last name)*

John L. Power

6. REPORT DATE	7a. TOTAL NO. OF PAGES	7b. NO. OF REFS
September 1973	46	21

8a. CONTRACT OR GRANT NO.	9a. ORIGINATOR'S REPORT NUMBER(S)
b. PROJECT NO.	4056
c.	9b. OTHER REPORT NO(S) *(Any other numbers that may be assigned this report)*
d.	

10. DISTRIBUTION STATEMENT

APPROVED FOR PUBLIC RELEASE: DISTRIBUTION UNLIMITED

11. SUPPLEMENTARY NOTES	12. SPONSORING MILITARY ACTIVITY

13. ABSTRACT

A three-dimensional smooth wall turbulent boundary layer with a moderate adverse pressure gradient was produced on the floor of a wind tunnel. The boundary layer velocity profile was measured at two positions, using a three-tube pressure probe. The streamwise, skin-friction coefficient was calculated with the skin-friction laws of Granville and Ludwieg and Tillmann using experimentally obtained boundary layer parameters. The results were compared with skin-friction coefficients obtained by using Preston tubes.

The calculated values of skin friction varied from agreement to 5 percent more than the Preston tube values. There is also evidence that the skewed flow in the boundary layer can affect Preston tube readings. It was concluded that the tunnel could be used to study boundary layers similar to those occurring on ships of moderate block coefficient.

DD FORM 1 NOV 65 1473 (PAGE 1)

S/N 0101-807-6801

UNCLASSIFIED

Security Classification

14. KEY WORDS	LINK A		LINK B		LINK C	
	ROLE	WT	ROLE	WT	ROLE	WT
Ship Resistance						
Ship Boundary Layers						
Turbulent Boundary Layers						